HHS Public Access

Author manuscript

Circ Res. Author manuscript; available in PMC 2019 May 25.

Published in final edited form as:

Circ Res. 2018 May 25; 122(11): 1501–1516. doi:10.1161/CIRCRESAHA.117.311872.

Cardiac Kir2.1 and $Na_V1.5$ Channels Traffic Together to the Sarcolemma to Control Excitability

Daniela Ponce-Balbuena[1], **Guadalupe Guerrero-Serna**[1], **Carmen R. Valdivia**[1], **Ricardo Caballero**[3,4], **F. Javier Diez-Guerra**[5], **Eric N. Jiménez-Vázquez**[1], **Rafael J. Ramírez**[1], **André Monteiro da Rocha**[1], **Todd J. Herron**[1], **Katherine F. Campbell**[1], **B. Cicero Willis**[1], **Francisco J. Alvarado**[6], **Manuel Zarzoso**[1], **Kuljeet Kaur**[1], **Marta Pérez-Hernández**[3,4], **Marcos Matamoros**[3,4], **Héctor H. Valdivia**[1,6], **Eva Delpón**[3,4], and **José Jalife**[1,2,*]

[1]Department of Internal Medicine and Center for Arrhythmia Research, University of Michigan, 2800 Plymouth Rd, Ann Arbor, MI 48109, USA

[6]Department of Molecular and Integrative Physiology, University of Michigan, 2800 Plymouth Rd, Ann Arbor, MI 48109, USA

[2]Centro Nacional de Investigaciones Cardiovasculares (CNIC), Madrid, Spain, and CIBERV

[3]Department of Pharmacology, School of Medicine, Universidad Complutense, 28040 Madrid, Spain

[4]Instituto de Investigación Sanitaria Gregorio Marañón. School of Medicine. Universidad Complutense. 28040 Madrid, Spain

[5]Departamento de Biología Molecular and Centro de Biología Molecular “Severo Ochoa” (UAM-CSIC), Universidad Autónoma de Madrid, 28049 Madrid, Spain

Abstract

Rationale—In cardiomyocytes, $Na_V1.5$ and Kir2.1 channels interact dynamically as part of membrane bound macromolecular complexes.

Objective—To test whether $Na_V1.5$ and Kir2.1 preassemble during early forward trafficking and travel together to common membrane microdomains.

Methods and Results—In patch-clamp experiments, co-expression of trafficking deficient mutants $Kir2.1^{\Delta 314–315}$ or $Kir2.1^{R44A/R46A}$ with wildtype (WT) $Na_V1.5^{WT}$ in heterologous cells reduced I_{Na}, compared to $Na_V1.5^{WT}$ alone or co-expressed with $Kir2.1^{WT}$. In cell surface biotinylation experiments, expression of $Kir2.1^{\Delta 314–315}$ reduced $Na_V1.5$ channel surface expression. Glycosylation analysis suggested that $Na_V1.5^{WT}$ and $Kir2.1^{WT}$ channels associate

Address correspondence to: Dr. José Jalife, Center for Arrhythmia Research, University of Michigan, NCRC, 2800 Plymouth Rd. Bldg. 26, Ann Arbor, MI, 48109, Tel. 734-998-7500, jjalife@umich.edu.

DISCLOSURES

None.

AUTHOR CONTRIBUTIONS

DP-B, GG-S, CRV, HHV, RC, ED, and JJ conceived experiments, designed research, and discussed results and strategy. DP-B, RC, FJD-G, ENJ-V, AMR, TJH, KFC, BCW, FJA, MZ, RJR, KK, MP-H, and MM performed experiments and collected, analyzed and discussed data; JJ directed the study. DP-B and JJ wrote the manuscript, which was revised and approved by all authors.

early in their biosynthetic pathway, and fluorescence recovery after photobleaching experiments demonstrated that co-expression with Kir2.1 increased cytoplasmic mobility of $Na_V1.5^{WT}$, and vice versa, whereas co-expression with $Kir2.1^{\Delta 314–315}$ reduced mobility of both channels. Viral gene transfer of $Kir2.1^{\Delta 314–315}$ in adult rat ventricular myocytes and human induced pluripotent stem cell-derived cardiomyocytes (hiPSC-CMs) reduced I_{K1} and I_{Na}, maximum diastolic potential (MDP) and action potential depolarization rate, and increased action potential duration (APD). Upon immunostaining, the adaptor protein complex 1 (AP1) colocalized with $Na_V1.5^{WT}$ and $Kir2.1^{WT}$ within areas corresponding to t-tubules and intercalated discs. Like $Kir2.1^{WT}$, $Na_V1.5^{WT}$ co-immunoprecipitated with AP1. Site-directed mutagenesis revealed that $Na_V1.5^{WT}$ channels interact with AP1 through the $Na_V1.5^{Y1810}$ residue, suggesting that, like for $Kir2.1^{WT}$, AP1 can mark $Na_V1.5$ channels for incorporation into clathrin-coated vesicles at the trans-Golgi. Silencing the AP1 ϒ-adaptin subunit in hiPSC-CMs reduced I_{K1}, I_{Na} and MPD, and impaired rate dependent APD adaptation.

Conclusions—The $Na_V1.5$-Kir2.1 macromolecular complex preassembles early in the forward trafficking pathway. Therefore, disruption of Kir2.1 trafficking in cardiomyocytes affects trafficking of $Na_V1.5$, which may have important implications in the mechanisms of arrhythmias in inheritable cardiac diseases.

Keywords

Ion channels; trafficking; electrophysiology; arrhythmias (mechanisms); protein trafficking arrhythmia

Subject Terms

Basic Science Research; Cell Signaling/Signal Transduction; Electrophysiology; Ion Channels/ Membrane Transport; Physiology

INTRODUCTION

In the human heart, three strong inward rectifying channels (Kir2.1, Kir2.2 and Kir2.3) contribute to the inward rectifier potassium current (I_{K1})[1]. I_{K1} is the major current responsible for maintenance of the maximum diastolic potential (MDP) in cardiomyocytes. It modulates excitability and influences the shape of the action potential (AP)[2–5]. Kir2.1 is the major channel isoform underlying I_{K1} in human ventricles, with Kir2.2 expressed to a lesser extent. In human atrial cells Kir2.3 is the main carrier of I_{K1}[6, 7].

An important aspect of Kir2.x channel regulation is precise forward trafficking to specific membrane subdomains[2, 7–9]. The Golgi acts as a central biosynthetic sorting station, responsible for directing newly synthesized membrane proteins to their appropriate subcellular destination[10, 11]. Signal-dependent Golgi export processes control membrane surface density of Kir2.x channels[12]. Transport of Kir2.1 channels from the Golgi is dictated by residues embedded in the NH_2 and COOH domains of the channel. These residues form a recognition site for interaction with adaptor protein complex 1 (AP1), thereby marking Kir2.1 for incorporation into clathrin-coated vesicles at the *trans*-Golgi[12].

Adaptor protein complexes are heterotetrameric protein complexes that mediate intracellular membrane trafficking. Of the five different adaptor protein complexes, AP1, AP2 and AP3 are clathrin-associated, whereas AP4 and AP5 are not[13]. The adaptor protein complexes bind to sorting signals on cytoplasmic tails of cargo proteins. They also recruit clathrin and other accessory proteins and concentrate cargo proteins into vesicular carriers that transport cargo proteins from donor to target membranes[13–15].

The voltage-gated cardiac sodium channel consists of a pore-forming alpha subunit ($Na_V1.5$) and one or more beta subunits that modulate, but are not crucial, for functional $Na_V1.5$ expression[16]. $Na_V1.5$ channels permeate inward sodium current (I_{Na}), which is the main depolarizing current in cardiomyocytes, and thus is critical for normal electrical conduction[16, 17]. Regulation of $Na_V1.5$ channel transport from Golgi to plasma membrane is poorly understood. Examination of $Na_V1.5$ glycosylation suggests the Na^+ channel can reach the plasma membrane via two different transport routes: the classical secretory transport route, or a Golgi-independent pathway[18].

Cellular processes that regulate trafficking and expression of Kir2.1 and $Na_V1.5$ channels are of interest as potential mediators of proarrhythmic channelopathies. Kir2.1 and $Na_V1.5$ can interact through common partners such as scaffolding, anchoring/adapter proteins, enzymes, and regulatory proteins[19–26]. We previously demonstrated that both channels belong to multi-protein complexes, enabling one to regulate the other's expression[22, 26, 27]. However, it remains unknown whether Kir2.1 and $Na_V1.5$ pre-assemble or interact during early trafficking steps of their secretory pathways.

Here we investigate whether Kir2.1 and $Na_V1.5$ associate early in their respective biosynthetic pathways, and whether they share a coupled forward trafficking process prior to formation of the $Na_V1.5$-Kir2.1 macromolecular complex at the cell membrane. We use trafficking-deficient mutant channels Kir2.1$^{\Delta 314–315}$ and Kir2.1$^{R44A/R46A}$ that disrupt Golgi trafficking of Kir2.1, thus impairing its surface expression[12, 28–31]. We hypothesize that expression of these trafficking-deficient Kir2.1 mutants will reciprocally disturb trafficking and functional expression of associated $Na_V1.5$ channels, consequently altering cellular excitability and establishing a substrate for arrhythmogenesis.

METHODS

The authors declare that all supporting data are available within the article [and its online supplementary files].

Expanded methodology can be found in Online Supplement.

Isolation and culture of cardiac myocytes

Calcium-tolerant adult rat ventricular myocytes (ARVMs) were isolated from hearts of normal adult male Sprague-Dawley rats. Cells were plated on laminin coated tissue culture glass coverslips/dishes and maintained in M199 for viral/non-viral transfer and patch clamping as previously described[32].

Cell culture and transfections

Human Embryonic Kidney (HEK-293T) cells were cultured in DMEM (Gibco) supplemented with fetal bovine serum (FBS), penicillin, and streptomycin at 37°C. HEK-293 cells stably expressing $Na_V1.5$+β1 channels were grown under the same conditions with the addition of Geneticin for selection of cells expressing the resistance marker. For patch-clamp experiments, cells were grown in 60 mm dishes and transfected or co-transfected using Lipofectamine.

iCell hiPSC-CM monolayers

Cryopreserved vials of human iCell® Cardiomyocytes were obtained from Cellular Dynamics International, Inc (Madison, WI). After 48 to 72 h of adenoviral overexpression electrophysiological phenotype analysis was performed.

Biotinylation assay

Forty-eight hours after transfection, HEK-293T cells were washed with phosphate-buffered saline and biotinylated for 60 min then incubated with glycine. Biotinylated proteins were analyzed by Western blot and immunoprecipitation assays.

Deglycosylation assay

Total membrane homogenates were solubilized and incubated with mouse anti-Kir2.1 antibody for immunoprecipitation. Samples were incubated with either PNGase-F, Endo-H or phosphate buffer and used for SDS-PAGE analysis.

I_{Na}, I_{K1} and AP recordings in ARVMs, hiPSC-CMs and HEK-293T cells

Voltage-clamp recordings were performed at room temperature and APs were recorded using current-clamp at 37°C.

Fluorescence recovery after photobleaching (FRAP)

$Na_V1.5^{WT}$ and $Kir2.1^{WT}$ channels were bound to mTurquoise (^{mTQ}) and venus (^{Venus}) fluorophores for FRAP experiments in COS-7 cells. Analysis was performed using Fiji/ImageJ and Matlab.

Statistics

All data are expressed as mean±SEM. Two-tail Student's *t*-test, One or Two-way ANOVA with Bonferroni's multiple comparison tests performed with Prism 6 were used. $p<0.05$ was considered significant.

RESULTS

Trafficking-deficient mutant $Kir2.1^{\Delta 314–315}$ impairs functional expression of $Na_V1.5$

We conducted patch-clamp experiments in transiently transfected HEK-293T cells. For $Kir2.1^{WT}$, voltage steps elicited the expected large inward and small outward currents of a strong inward rectifier channel. In contrast, no potassium current was detected for the trafficking-deficient mutant $Kir2.1^{\Delta 314–315}$ (Online Figure I A,B), as previously reported[28].

In addition, we confirmed previous data showing cooperative interaction between $Kir2.1^{WT}$ and $Na_V1.5^{WT}$ ion channel expression[22, 26, 27]. We observed a synergistic effect on $I_{Nav1.5}$ density when $Kir2.1^{WT}$ channels were co-expressed (1:1) with $Na_V1.5^{WT}$ channels, resulting in increased $I_{Nav1.5}$. Co-expression of $Kir2.1^{WT}$ channels with $Na_V1.5^{WT}$ channels resulted in larger peak $I_{Nav1.5}$ density at −25 mV compared with $Na_V1.5^{WT}$ alone (−830±65 pA/pF *versus* −562±57 pA/pF, respectively; p=0.001, Online Figure I C,D). We also assessed functional consequences on $I_{Kir2.1}$ of co-expressing $Na_V1.5^{WT}$ with the trafficking-deficient $Kir2.1^{\Delta 314–315}$ channel. No $I_{Kir2.1}$ density was generated by $Kir2.1^{\Delta 314–315}$ channels when co-expressed with $Na_V1.5^{WT}$ channels. Co-expression of $Kir2.1^{WT}$, $Kir2.1^{\Delta 314–315}$ and $Na_V1.5^{WT}$ (0.5:0.5:1) yielded an $I_{Kir2.1}$ density that was 92% smaller than when $Kir2.1^{WT}$ was expressed alone (Online Figure I A,B).

We then co-expressed $Na_V1.5^{WT}$ with $Kir2.1^{\Delta 314–315}$ and measured $Na_V1.5^{WT}$ channel function. $I_{Nav1.5}$ density in cells with $Na_V1.5^{WT}$ channels expressed alone was larger than in cells that co-expressed $Kir2.1^{\Delta 314–315}$, with peak currents at −25 mV of −562±57 *versus* −275±38 pA/pF, respectively (p<0.0001, Online Figure I C,D). Correspondingly, $I_{Nav1.5}$ density in cells with $Na_V1.5^{WT}$ channels expressed alone was larger than in cells that co-expressed $Kir2.1^{WT}$, $Kir2.1^{\Delta 314–315}$ and $Na_V1.5^{WT}$ subunits (peak current at −25 mV, −562±57 *versus* −178±34 pA/pF, respectively, p<0.0001, Online Figure I C,D).

To rule out the possibility that decreased $I_{Nav1.5}$ density in the presence of the trafficking-deficient mutant $Kir2.1^{\Delta 314–315}$ was due to variability in expression from transfection, we used a stable HEK-293 cell line expressing $Na_V1.5$+β1. Cells transfected with $Kir2.1^{\Delta 314–315}$ had a lower $I_{Nav1.5}$ than control GFP-transfected cells. Cells transfected with $Kir2.1^{\Delta 314–315}$ exhibited smaller $I_{Nav1.5}$ density −244±37 pA/pF than control GFP-transfected cells −373±50 pA/pF at −25 mV, p<0.003. On the other hand, cells transfected with $Kir2.1^{WT}$ had a larger mean I_{Na} peak density −520±69 pA/pF at −25 mV than control cells, p<0.0001, Online Figure II A,B and Online Table I. We observed no differences in voltage-dependence of activation or inactivation, or recovery from inactivation between groups (Online Figure III A-D and Online Table I).

Thus, trafficking deficiency of one channel component of the $Na_V1.5$-Kir2.1 macromolecular complex (in this case $Kir2.1^{\Delta 314–315}$) negatively influenced functional expression of the other channel ($Na_V1.5$), possibly by disturbing channel trafficking to the plasma membrane.

Double mutant $Kir2.1^{R44A/R46A}$ reduces $I_{Nav1.5}$ density in CHO cells

To explore whether other trafficking-deficient Kir2.1 channels can produce similar effects on $I_{Nav1.5}$ density, we studied the NH_2 double mutant $Kir2.1^{R44A/R46A}$, which accumulates in the Golgi resulting in decreased membrane expression[33]. Surprisingly, patch-clamp experiments in HEK-293T and CHO cells showed that the $Kir2.1^{R44A/R46A}$ mutant produced an $I_{Kir2.1}$ density similar to $Kir2.1^{WT}$ channels (Online Figure IV A,B). However, we observed that in transfected CHO cells, $I_{Nav1.5}$ density of $Na_V1.5^{WT}$ channels expressed alone was larger than in cells that co-expressed $Kir2.1^{R44A/R46A}$ (Online Figure II C,D). Thus, decreased $I_{Nav1.5}$ density was not unique to $Kir2.1^{\Delta 314–315}$ channels, as other Kir2.1 trafficking-deficient mutants in a different cell line produced similar effects.

Kir2.1$^{\Delta 314–315}$ expression reduces I_{Na} density in adult rat ventricular myocytes (ARVMs)

We next studied the functional consequences of expressing Kir2.1$^{\Delta 314–315}$ in adult mammalian cardiac cells. Using an adenoviral construct, we overexpressed Ad-Kir2.1$^{\Delta 314–315}$ in ARVMs; control myocytes were infected with GFP (Ad-GFP). Cell capacitance was similar in myocytes infected with Ad-Kir2.1$^{\Delta 314–315}$ and control Ad-GFP myocytes (100±5 versus 107±2 pF; n=27, n=23; respectively; p=0.4). Representative Ba^{2+} sensitive I_{K1} traces from Ad-GFP and Ad-Kir2.1$^{\Delta 314–315}$ are shown in Figure 1A. Figure 1B shows the I_{K1} current-voltage relationship for Ad-GFP and Ad-Kir2.1$^{\Delta 314–315}$. As expected, ARVMs transfected with Ad-Kir2.1$^{\Delta 314–315}$ generated smaller inward −3±0.4 *versus* −10±8 pA/pF at −120 mV; $p<10^{-7}$ and outward 0.15±0.01 *versus* 0.5±0.06 pA/pF at −60 mV, $p<10^{-5}$ currents than control. We next investigated functional effects of Ad-Kir2.1$^{\Delta 314–315}$ overexpression on I_{Na} in myocytes. Representative I_{Na} traces from Ad-GFP and Ad-Kir2.1$^{\Delta 314–315}$ are in Figure 1C. Overexpression of Kir2.1$^{\Delta 314–315}$ decreased I_{Na} density compared with Ad-GFP, Figure 1D. Mean peak current density at −35 mV was −39±3 *versus* −52±4 pA/pF, respectively, p=0.05.

To evaluate whether overexpression of Kir2.1$^{\Delta 314–315}$ in ARVMs could affect other currents, like transient outward potassium current (I_{to}), we compared the difference between initial peak and sustained K^+ background current density of myocytes infected with Ad-Kir2.1$^{\Delta 314–315}$ versus Ad-GFP cells. Peak currents at 30 mV were 8.1±1 *versus* 7.5±1 pA/pF, respectively, p=0.79. In contrast with the decrease in I_{K1}, Ad-Kir2.1$^{\Delta 314–315}$ expression did not modify I_{to} (Online Figure V).

Kir2.1$^{\Delta 314–315}$ expression modifies ARVM cardiac action potential

We studied cellular electrophysiological consequences of Kir2.1$^{\Delta 314–315}$ expression by recording APs in Ad-Kir2.1$^{\Delta 314–315}$-infected ARVMs. As expected, the MDP was reduced compared to control (−66±3 *versus* −79±1 mV; p=0.0028; Figure 2A,C). MDP decrease was consistent with I_{K1} reduction (Figure 1A,B). In some Ad-Kir2.1$^{\Delta 314–315}$-infected ARVMs, MDP reduction resulted in phase-4 depolarization and generation of spontaneous APs (Online Figure VI). In addition, maximum upstroke velocity (dV/dt_{max}) was reduced in Ad-Kir2.1$^{\Delta 314–315}$ myocytes compared to control 91±2 *versus* 184±1 V/s, respectively; p=0.012, Figure 2D. These findings were in agreement with reduction in both sodium channel availability during the AP upstroke and I_{Na} density in Ad-Kir2.1$^{\Delta 314–315}$ myocytes (Figure 1C,D). Moreover, APD was prolonged in Ad-Kir2.1$^{\Delta 314–315}$ (Figure 2E). Finally, we observed no difference in AP overshoot between control and Ad-Kir2.1$^{\Delta 314–315}$ myocytes (Figure 2F).

Kir2.1$^{\Delta 314–315}$ mutant decreases I_{K1} and I_{Na} in hiPSC-CMs

We determined the consequences of expression of Kir2.1$^{\Delta 314–315}$ in hiPSC-CMs by adenoviral infection; control cells were infected with Ad-GFP. Figure 3A shows representative Ba^{2+} sensitive I_{K1} traces for Ad-GFP and Ad-Kir2.1$^{\Delta 314–315}$. Control I_{K1} current-voltage relationship is plotted with the Ad-Kir2.1$^{\Delta 314–315}$ curve. As expected, hiPSC-CMs infected with Ad-Kir2.1$^{\Delta 314–315}$ generated smaller currents than control −0.8±0.3 *versus* −3.6±0.6 pA/pF at −120 mV, p=0.006, Figure 3B. We next investigated the functional effects of Ad-Kir2.1$^{\Delta 314–315}$ overexpression on I_{Na} in human myocytes.

Representative I_{Na} traces are shown in figure 3C. In figure 3D, overexpression of Kir2.1$^{\Delta 314–315}$ decreased I_{Na} density at several test voltages compared with Ad-GFP. Peak currents at −20 mV were −14±1 *versus* −21±2 pA/pF, respectively, p=0.014.

Kir2.1$^{\Delta 314–315}$ does not alter total $Na_V1.5$ protein levels but impairs $Na_V1.5$ plasma membrane expression

We observed no change in total $Na_V1.5^{WT}$ protein expression in whole-cell extracts of HEK-293 ($Na_V1.5+\beta1$) transfected with either Kir2.1^{WT} or mutant Kir2.1$^{\Delta 314–315}$ protein, p=0.14. Similar results were obtained in HEK-293T cells transiently transfected with $Na_V1.5$ alone or co-transfected with either Kir2.1^{WT} or mutant Kir2.1$^{\Delta 314–315}$, p=0.25, Online Figure VII B,E. Moreover, as previously, we observed less total protein production of Kir2.1$^{\Delta 314–315}$ than Kir2.1^{WT} channel[12, 28, 34] (Online Figure VII C,F). Therefore, to determine whether the decrease in I_{Na} density in cells co-expressing Kir2.1$^{\Delta 314–315}$ was due to a decrease in $Na_V1.5^{WT}$ surface membrane expression, we performed cell surface biotinylation experiments in HEK-293T cells after transient co-transfection 1:1 of $Na_V1.5^{WT}$ with Kir2.1^{WT} or Kir2.1$^{\Delta 314–315}$ channels. Cell lysates were subjected to immunoprecipitation with an antibody against the COOH-domain of $Na_V1.5$ and analyzed by Western blotting. The presence of the trafficking-deficient mutant Kir2.1$^{\Delta 314–315}$ resulted in a reduction in $Na_V1.5^{WT}$ protein at the surface membrane compared with Kir2.1^{WT} channel, p=0.009, Figure 4A,B.

$Na_V1.5$ and Kir2.1 associate early in their biosynthetic pathway

$Na_V1.5$ and Kir2.1 channels are present as complexes together with scaffolding proteins[19–26], and co-immunoprecipitate in both forward and reverse co-immunoprecipitation reactions[22]. However, the spatial and temporal coordination of their association remains unclear regarding $Na_V1.5$ and Kir2.1 coupling before, during or after insertion into the membrane. To determine whether association occurs before the channels reach the plasma membrane we examined their sensitivity to Endoglycosidase-H (Endo-H), which cleaves high mannose carbohydrates and indicates association with the endoplasmic reticulum (ER)-Golgi apparatus[35]. Whole-cell homogenates and immunoprecipitates from HEK-293T cells co-transfected 1:1 with $Na_V1.5^{WT}$ and Kir2.1^{WT} channels were analyzed by Western blot after treatment with Endo-H or Peptide-*N*-Glycosidase-F (PNGase-F), which enzymatically removed glycans added in the ER or all *N*-linked carbohydrates, respectively (Figure 4C). $Na_V1.5^{WT}$ channels that co-immunoprecipitated with Kir2.1^{WT} channels were partially Endo-H-sensitive, as evidenced by the appearance of a lower molecular weight band after Endo-H treatment. The positive association between Endo-H-sensitive $Na_V1.5^{WT}$ and Kir2.1^{WT} channels suggested that the $Na_V1.5$-Kir2.1 complex assembly occurred at least partially when the two channels trafficked through the ER-Golgi. Moreover, in co-immunoprecipitation experiments using an antibody against Nav1.5 in cells co-transfected with $Na_V1.5^{WT}$ and Kir2.1^{WT} or Kir2.1$^{\Delta 314–315}$, Nav1.5^{WT} was able to pull down both Kir2.1^{WT} and mutant Kir2.1$^{\Delta 314–315}$ (Online Figure VIII). Taken together, these data indicate that $Na_V1.5$ and Kir2.1 channels can associate early in their biosynthetic pathway.

Kir2.1^{WT} increases while Kir2.1$^{\Delta 314–315}$ impairs $Na_V1.5$ mobility toward plasma membrane

We conducted fluorescence recovery after photobleaching (FRAP) experiments to assess whether Kir2.1 and $Na_V1.5$ traffic together along a common pathway. We subcloned each channel gene with one of two separate fluorophores (*SCN5A* with mTq2, and *KCNJ2* or *KCNJ2*$^{\Delta 314–315}$ with Cp173venus), then used confocal microscopy and FRAP to quantify channel mobility when transfected alone or co-transfected together into COS-7 cells. After photobleaching a small region of interest (ROI = 5 μm diameter), the rate of fluorescence recovery was measured as an index of movement of unbleached channels entering the ROI. Online Figure IX A shows FRAP data for Kir2.1$^{WT\ Venus}$ alone and for Kir2.1^{WT} co-transfected with $Na_V1.5^{WT\ mTQ}$. Presence of $Na_V1.5^{WT\ mTQ}$ channels did not modify the fraction of mobile Kir2.1$^{WT\ Venus}$ channels (Online Figure IX B), but accelerated the fluorescence recovery within the ROI $t_{1/2}$= 2.3±0.3 min (n=8) *versus* 4.7±0.6 min (n=7); p=0.002. These changes are better appreciated in Online Figure IX C, which shows Kir2.1$^{WT\ Venus}$ recovery normalized to the maximum fluorescence recorded after photobleaching in the absence and the presence of $Na_V1.5^{WT\ mTQ}$. The mobile fraction of $Na_V1.5^{WT\ mTQ}$ channels increased when co-transfected with Kir2.1$^{WT\ Venus}$ (Online Figure IX D-F), although its $t_{1/2}$ was not modified $t_{1/2}$=2.4±0.2 min (n=11) *versus* 2.0±0.2 min (n=10), respectively; p=0.17. The mobile fraction and $t_{1/2}$ for both $Na_V1.5^{WT\ mTQ}$ and Kir2.1$^{WT\ Venus}$ channels were nearly identical when measurements were performed in the presence of the other channel (i.e. $Na_V1.5^{WT\ mTQ}$ and Kir2.1$^{WT\ Venus}$, and vice versa; Online Figure IX G-I). Furthermore, co-transfection with Kir2.1$^{\Delta 314–315Venus}$ decreased the mobile fraction, $p<0.005$, Online Figure IX E and delayed recovery of $Na_V1.5^{WT\ mTQ2}$ channels $t_{1/2}$=3.1±0.4 min, n=9, p=0.11, Online Figure IX D-F. Altogether, the results strongly suggest that Kir2.1^{WT}-$Na_V1.5^{WT}$ complexes travel more efficiently than $Na_V1.5^{WT\ mTQ2}$ channels alone and faster than Kir2.1$^{WT\ Venus}$ channels alone, and that the presence of Kir2.1$^{\Delta 314–315Venus}$ reduces both the amount and rate of $Na_V1.5^{WT\ mTQ}$ channel protein trafficking.

Localization of AP1 ϒ-adaptin subunit in ARVMs

Forward protein trafficking along intracellular compartments is accomplished by transport vesicles that form at sites where coat proteins have been recruited[15, 36]. Previously it was shown that an interaction with the AP1 ϒ-adaptin subunit marks the incorporation of Kir2.1^{WT} channels into clathrin coated vesicles at the *trans* Golgi network[12]. Also previous studies have shown that Kir2.1 and $Na_V1.5$ channels present similar subcellular distributions at t-tubules and the intercalated discs[7, 20–22, 26, 37, 38] We therefore sought to determine whether in addition to Kir2.1, AP1 ϒ-adaptin also interacts with $Na_V1.5$ in ARVM. On the top panel of Figure 5, immunostaining with an antibody against AP1 ϒ-adaptin, shows a striated and punctate pattern distributed within regions corresponding to the t-tubules and the intercalated discs. Magnifications of the box region (panels a-g) shows that AP1 ϒ-adaptin colocalizes with $Na_V1.5$ and Kir2.1 channels at both the t-tubular regions and more intensely the intercalated discs (panels d,f and g).

$Na_V1.5$ Golgi export depends on interaction with the AP1 ϒ-adaptin subunit clathrin adaptor complex

Next, we conducted co-immunoprecipitation experiments to investigate whether, similar to $Kir2.1^{WT}$, $Na_V1.5^{WT}$ protein interacts with the AP1 ϒ-adaptin subunit. We used an antibody against the COOH-domain of $Na_V1.5$ for immunoprecipitation from whole-cell homogenates of HEK-293T cells transfected with $Na_V1.5^{WT}$ alone or co-transfected 1:1 with $Kir2.1^{WT}$ or $Kir2.1^{\Delta 314–315}$. Immunoprecipitated proteins were prepared for Western blot analysis and probed with anti-AP1 ϒ-adaptin monoclonal antibody. As illustrated in Online Figure X A and B, $Na_V1.5$ channels pulled down AP1 ϒ-adaptin; the reverse interaction demonstrated that AP1 was also able to pull down $Na_V1.5$ in immunoprecipitation experiments. Since selective recruitment of the coat protein is based on sequence information within the cytoplasmic domains of the respective cargo protein[33, 39–44], we next investigated whether the $Na_V1.5$ COOH and/or NH_2 domains contained the typical consensus motif ($YXX\Phi$; X being any amino acid and Φ being a bulky, hydrophobic residue) for adaptin binding. In the COOH-domain of $Na_V1.5$ channels we found four consensus motifs for AP1 binding, beginning at amino acid positions Y1794, Y1810, Y1888 and Y1976. In the NH_2 domain one consensus motif for AP1 begins at amino acid position Y68. We therefore subjected the Tyrosine (Y) residues of the consensus motifs to sequential Alanine (A) replacement mutagenesis and assessed whether the mutant $Na_V1.5$ channels interacted with the AP1 ϒ-adaptin subunit and whether they were functional. Immunoblots of all Alanine-substitutions ($Na_V1.5^{Y68A}$, $Na_V1.5^{Y1810A}$, $Na_V1.5^{Y1888A}$ and $Na_V1.5^{Y1976A}$) showed a band at ~250 KDa in all inputs and co-immunoprecipitation samples from $Na_V1.5$ mutants and $Na_V1.5^{WT}$ channels (Figure 6A). No change in total protein expression was observed between AP1 binding mutant consensus motifs and the $Na_V1.5^{WT}$ channel (Online Figure XI A,B). Moreover, all Alanine-substitutions expressed functional $Na_V1.5$ channels (Figure 6B). However, I_{Na} density was reduced for the $Na_V1.5^{Y1810A}$ mutant (Figure 6B,C). This result was consistent with the observed loss of interaction between $Na_V1.5^{Y1810A}$ and the AP1 ϒ-adaptin subunit (Figure 6A). Taken together, the data suggest that similar to Kir2.1, a significant proportion of $Na_V1.5$ channels interact with AP1 and are selected for export from the Golgi in a signal dependent manner through an AP1 clathrin adaptor interaction.

Silencing the AP1 ϒ-adaptin subunit reduces I_{Na}, I_{K1} and modifies the action potential characteristics of hiPSC-CMs

We used adenoviral transfer technology to knock down the expression of AP1 ϒ-adaptin subunit and measured I_{Na} and I_{K1} densities in hiPSC-CMs. We cultured hiPSC-CM monolayers for 7 days on 96-well plates as describe previously.[45] hiPSC-CM monolayers were infected with shRNA for AP1 ϒ-adaptin (Ad-shϒ-adaptin) at varying MOIs to determine the level needed for knockdown; samples were collected 3 days postinfection. Separate groups of hiPSC-CM monolayers were infected with control Scramble-GFP virus (Ad-Scr-GFP), Online Figure XII A,B. On Western Blot analysis, 200 MOI reduced relative levels of AP1 ϒ-adaptin protein by ~63 % without suppressing total $Na_V1.5^{WT}$ or $Kir2.1^{WT}$ protein levels (Figure 7A,B). I_{K1} density was smaller in hiPSC-CMs infected with Ad-shϒ-adaptin compared with control GFP infected hiPSC-CMs (−9.3±1.7 *versus* −3.8±0.5 pA/pF at −120 mV, p=0.01, Figure 7C,D). Similar to I_{K1}, infection with Ad-shϒ-adaptin also

reduced I_{Na} density compared to Ad-Scr-GFP. Peak currents at −20 mV were −18±1 *versus* −24±1 pA/pF, respectively, p=0.004, Figure 7E,F.

Next, we determined the effect of silencing the AP1 ϒ-adaptin subunit on the action potential characteristics of hiPSC-CMs. In Figure 8F, MDP was reduced in hiPSC-CMs treated with Ad-shϒ-adaptin relative to control hiPSC-CMs infected with Ad-Scr-GFP. All cells were paced at 2.5 and 5 Hz. MDPs were −68±1 (2.5 Hz) and −68±1 mV (5 Hz) in Ad-shϒ-adaptin hiPSC-CMs, *versus* −79±2 (2.5 Hz) and −78±2 mV (5 Hz) in Ad-Scr-GFP iPSC-CMs (p=0.01 in both cases). Action potential amplitude, APD_{50}, APD_{90}, dV/dt_{max} and overshoot, were similar in both hiPSC-CMs groups (Figure 8 B,C,D,G,H). Silencing the AP1 ϒ-adaptin subunit impaired the rate dependent APD adaptation of hiPSC-CMs, ΔAPD_{90}, ΔAPD_{50} were 2±4, 1±4 ms, respectively, in iPSC-CMs Ad-shϒ-adaptin *versus* 20±4, 18±4 ms in iPSC-CMs Ad-Scr-GFP, respectively, p=0.04 for both ΔAPD, Figure 8E.

DISCUSSION

We used two trafficking-deficient mutant Kir2.1 channels to provide novel insight into mechanisms that regulate the $Na_V1.5$-Kir2.1 macromolecular complex. Our data reveal that co-expression with $Kir2.1^{\Delta 314–315}$ reduces expression of $Na_V1.5$ at the surface membrane without modifying biophysical properties of the channel or total protein production. We show that $Na_V1.5$ and Kir2.1 channels can associate early in their biosynthetic pathway, and that the $Na_V1.5$-Kir2.1 complex traffics more efficiently than $Na_V1.5$ alone, but $Kir2.1^{\Delta 314–315}$ impairs $Na_V1.5$ trafficking. Correspondingly, our patch-clamp data demonstrate that reduced $Na_V1.5$ surface membrane expression results in decreased I_{Na} density. In both ARVMs and hiPSC-CMs expression of mutant $Kir2.1^{\Delta 314–315}$ channel reduced I_{K1} and I_{Na}, MDP and dV/dt_{max}, and increased APD. In immunostaining experiments AP1 ϒ-adaptin shows a t-tubular distribution and is also concentrated at the intercalated disc colocalizing with both $Na_V1.5$ and Kir2.1. Site-direct mutagenesis revealed that $Na_V1.5^{WT}$ interacts with AP1 ϒ-adaptin through the $Na_V1.5^{Y1810}$ residue. Finally, silencing the AP1 ϒ-adaptin subunit in hiPSC-CMs reduced I_{K1}, I_{Na} and MDP, and impaired rate dependent APD adaptation. These data suggest strongly that in cardiomyocytes, $Na_V1.5$ and Kir2.1 channels may travel together to their eventual micro-domains, whether at the lateral membrane, t-tubule or intercalated disc; disruption of Kir2.1 trafficking affects trafficking of $Na_V1.5$; and Golgi export of a proportion of $Na_V1.5^{WT}$ channels depends on interaction with the AP1 ϒ-adaptin subunit clathrin adaptor complex. The $Kir2.1^{\Delta 314–315}$ mutant is expressed and processed into mature channels but at much lower efficiency than $Kir2.1^{WT}$;[12, 28, 34] we observed less total protein production for $Kir2.1^{\Delta 314–315}$ than $Kir2.1^{WT}$ (Online Figure VII C,F). Nevertheless, $Kir2.1^{\Delta 314–315}$ was sufficient to affect trafficking of $Na_V1.5$ to the cell surface whether it was expressed to form homotetramers, or to form heterotetramers with $Kir2.1^{WT}$ (Figure 1C,D, Figure 3C,D, Online Figure I C,D and Online Figure II B). Further, when we co-transfected $Kir2.1^{WT}$, $Kir2.1^{\Delta 314–315}$ and $Na_V1.5^{WT}$, the $I_{Kir2.1}$ density was 92% smaller than the $I_{Kir2.1}$ density of $Kir2.1^{WT}$ when expressed alone. These results agree with previous reports showing that, while $Kir2.1^{\Delta 314–315}$ forms channels that do not traffic to the membrane surface, they retain their ability to co-assemble with, and exert a dominant negative effect on the $Kir2.1^{WT}$ channels.[28] Therefore, it is possible that the $I_{Kir2.1}$ density recorded is elicited by $Kir2.1^{WT}$ subunits

co-assembled as homotetramers rather than $Kir2.1^{WT}$ or $Kir2.1^{\Delta 314–315}$ subunits rescued by the expression by $Na_V1.5^{WT}$ channels, Online Figure I A,B.

Expression of the trafficking-deficient mutant $Kir2.1^{\Delta 314–315}$ channel significantly reduced I_{Na} density in HEK-293T cells, ARVMs and hiPSC-CMs. However, a significant amount of residual current was maintained in all cases, implying that some $Na_V1.5$ channels were able to reach the plasma membrane. Data in the literature suggest that HEK-293 cells, cardiomyocytes and developing neurons contain multiple intracellular storage pools of $Na_V1.5$ channel protein that can be mobilized following a physiologic stimulus[46–48]. Those reports together with our data suggest that different pools of $Na_V1.5$ channels reach the plasma membrane from distinct origins (Golgi apparatus, unconventional Golgi pathway or storage pools). Based on the report by Mercier and coworkers[18], as well as our results, it is likely that the $Na_V1.5$ channels affected by $Kir2.1^{\Delta 314–315}$ are nascent $Na_V1.5$ channels that use the classical Golgi secretory route to reach the plasma membrane. The percentage of $Na_V1.5$ channels that use one or the other pathway remains a topic of further experimentation. Even so, the fact that a fraction of $Na_V1.5^{WT}$ channels that associate with $Kir2.1^{WT}$ are Endo-H-sensitive, strongly suggests that $Na_V1.5^{WT}$ and $Kir2.1^{WT}$ channels can interact early in their biosynthetic pathway.

Our understanding of how newly synthesized plasma membrane proteins are sorted to the cell membrane is still limited. Critical regulatory steps that control the surface expression of ion channels are likely to be involved starting at the endoplasmic reticulum and Golgi. Considerable evidence indicates that targeting or trafficking of ion channels within the cell is frequently mediated by interaction with other proteins through specific amino acid motifs present in the channel sequence[20–23, 26, 38, 49]. Moreover, evidence suggests the existence of retention and export trafficking signals that regulate functional expression of transmembrane proteins[33, 39–44]. Still, the precise export signals that regulate exit of $Na_V1.5$ from the Golgi and transit to the plasma membrane are not fully understood. The AP1 clathrin adaptor is one of the best known molecules to facilitate export of cargo proteins from the *trans*-Golgi network[50]. We show the distribution of AP1 protein and its colocalization with $Na_V1.5$ and Kir2.1 in cardiac cells and explored whether $Na_V1.5$ contained the typical amino acid consensus motif sequence ($YXX\Phi$) for adaptin binding. Based on the amino acid sequence of the channel we identified four probable consensus binding motifs for the AP1 complex on the COOH domain (Y1794, Y1810, Y1888, Y1976) and one possible motif on the NH_2 domain (Y68). Furthermore, our co-immunoprecipitation experiments demonstrate that $Na_V1.5$ interacts with the AP1 complex. Yet $Na_V1.5^{Y1810A}$ did not co-immunoprecipitate with AP1 protein, consistent with a decrease in I_{Na} density flowing through $Na_V1.5^{Y1810A}$ channels. This suggests that, similar to Kir2.1, some $Na_V1.5$ channels may be exported from the Golgi in a signal-dependent manner through an AP1 clathrin adaptor interaction. We observed that $Na_V1.5^{Y1976A}$ channels had an increased I_{Na} density relative to control. Interestingly the Y1976 residue locates within the PY motif of the $Na_V1.5$ channel,[51, 52] and the $Na_V1.5^{Y1976A}$ mutant has been shown to impair the Nedd4-2 binding motif[53]. Therefore, it is likely that the increase in I_{Na} density observed for the $Na_V1.5^{Y1976A}$ mutant is the result of decreased ubiquitination followed by internalization and/or degradation of $Na_V1.5^{Y1976A}$ channels. Future studies will be necessary to confirm that hypothesis.

It has been proposed that the Y*XX*Φ consensus motif recruits specific coat protein complexes that induce formation of transport vesicles, not only destined for certain subcellular localization, but also preferentially loaded with respective cargo proteins[54]. Thus, based on our data showing that both channels interact with the AP1 complex, we postulate that Kir2.1 and $Na_V1.5$ channels may be loaded in joint transport vesicles to be delivered to common subdomains at the plasma membrane. These data support previous reports on the existence of different pools of $Na_V1.5$ channel trafficking vesicles[18] and suggest that trafficking vesicles may carry varying compositions of load proteins. However, even though our data show $Na_V1.5$ can interact with AP1 for transportation, we cannot exclude participation of GGA1, a protein also known to facilitate export cargo from the *trans*-Golgi network[50].

Moreover, we observed that silencing the AP1 ϒ-adaptin subunit in hiPSC-CMs reduced I_{K1}, I_{Na} and the MDP and impaired the rate dependent APD adaptation. However, significant amounts of residual I_{K1} and I_{Na} were maintained, implying that some Kir2.1 and $Na_V1.5$ channels reached the plasma membrane. These data suggest that, like $Na_V1.5$ channels, Kir2.1 channels reach the plasma from distinct origins that may include, in addition to the Golgi apparatus, an unconventional Golgi pathway or storage pools and that other proteins may be involved in the export of Kir2.1 and $Na_V1.5$ channels from the *trans*-Golgi network. The observation that AP1 ϒ-adaptin silencing impaired the rate dependence of APD adaptation in hiPSC-CMs, suggests that AP1 ϒ protein may regulate the expression of ion channels and proteins involved in calcium homeostasis[55–58].

The intracellular COOH terminal of $Na_V1.5$ contains several protein-protein interaction motifs. The most well-characterized interaction sites are the calmodulin-biding IQ motif, the PY motif, and a PDZ domain-biding motif[59, 60]. In contrast, less is known about proteins that interact with the NH_2 domain of $Na_V1.5$. The $Na_V1.5$ NH_2 domain is critical for expression density, although the specific mechanism is not clear. A putative $Na_V1.5$ NH_2 fragment enhances $Na_V1.5^{WT}$ channel trafficking by possibly acting as a decoy, allowing $Na_V1.5^{WT}$ channels to bypass a regulatory system and reach the plasma membrane[61]. More recently, Matamoros *et al.* demonstrated that the NH_2 terminus of $Na_V1.5$ has a PDZ-like binding domain that mediates binding to α1-syntrophin, and can act like a chaperone to increase I_{Na} and I_{K1} through enhanced expression of $Na_V1.5$, Kir2.1, and Kir2.2 but not Kir2.3 proteins[26].

Our data demonstrate for the first time that $Na_V1.5$ interact with AP1 involved in the *trans*-Golgi network of cargo export proteins. Similar to the Kir2.1-AP1 complex[12], the $Na_V1.5$-AP1 complex interaction may participate in regulation of functional expression of $Na_V1.5$, and contribute to formation of the $Na_V1.5$-Kir2.1 channelosome[22]

Clinical relevance

The interplay between I_{K1} and I_{Na} is crucial to normal cardiac electrical function. By controlling resting membrane potential, I_{K1} modifies sodium channel availability and therefore cell excitability, APD, and conduction velocity. I_{K1} and I_{Na} interactions are key determinants of electrical rotor dynamics which are responsible for abnormal, often lethal, cardiac reentrant activity[62]. Data presented here demonstrate that expression of the

trafficking-deficient mutant Kir2.1$^{\Delta 314–315}$ in myocytes not only reduces native I_{K1}, but also I_{Na} by disrupting functional expression of both channels at the plasma membrane. Previous simulation studies predicted that a reduction in I_{K1} might have unique effects on AP configuration and arrhythmia susceptibility[30]. It was anticipated that a reduction in I_{K1} would prolong the terminal repolarization phase of the cardiac AP by reducing the amount of repolarizing current during the terminal phase of the AP, resulting in QT prolongation in affected individuals[30]. It is well known that AP prolongation is a prerequisite for early afterdepolarizations that can trigger spontaneous APs. In ARVMs we observed that expression of Kir2.1$^{\Delta 314–315}$ resulted in membrane depolarization, marked APD prolongation and spontaneous APs, validating the aforementioned numerical predictions.

Andersen-Tawil Syndrome type 1 (ATS1) is a rare disorder caused by mutations in the *KCNJ2* gene coding Kir2.1. Clinical manifestations of ATS1 include periodic paralysis, cardiac arrhythmias, and dysmorphic features. The cardiac manifestations of ATS1 patients with *KCNJ2* mutations include QT prolongation, premature ventricular contractions, complex ventricular ectopy, bigeminy, and polymorphic or bidirectional ventricular tachycardia. It has been difficult to correlate functional consequences of individual Kir2.1 mutation12 s with corresponding clinical phenotypes[28–30, 63]. Our data provide novel insights into the ionic basis of arrhythmia susceptibility in ATS1 patients. We postulate that in addition to reduced I_{K1}, ATS1 patients also have reduced I_{Na} as a consequence of disruption of the Kir2.1-$Na_V1.5$ complex by a trafficking-deficient Kir2.1 mutation. Consequently, co-expression of the trafficking-deficient mutant Kir2.1 channel with $Na_V1.5^{WT}$ is expected to contribute to arrhythmogenesis in ATS1 patients by reducing MDP and dV/dt_{max} via two different mechanisms: the voltage dependent mechanism, and effects of physical intermolecular interactions between the two channels. Our data highlight the importance of considering effects of a given mutation on functional expression of other ion channels or proteins that may be a part of the macromolecular complex within which Kir2.1 interacts.

Our study focused on the interplay between Kir2.1 and $Na_V1.5$. However, it is likely that other proteins, including ion channels, are part of the same macromolecular complex. The presence of a trafficking-deficient mutant channel may have the potential to affect functional expression of another channel within its macromolecular complex. Notably, we selected Kir2.1$^{\Delta 314–315}$ for its ability to retain the channel in the Golgi and its strong dominant negative effect. We also explored functional consequences of co-expressing $Na_V1.5$ with the double mutant Kir2.1$^{R44A/R46A}$, whose surface expression is reduced[33]. We observed that $I_{Nav1.5}$ density of cells that co-expressed Kir2.1$^{R44A/R46A}$ was reduced with respect to cells expressing $Na_V1.5^{WT}$ channels alone (Online Figure II C,D). Unexpectedly, our functional analysis showed that mutant Kir2.1$^{R44A/R46A}$ channels generated a current density that was similar to $I_{Kir2.1}{}^{WT}$. Future studies will be necessary to further elucidate the molecular mechanism involved in the regulation of functional expression of Kir2.1 channels.

These data support our contention that a common early anterograde trafficking mechanism is involved in transport of $Na_V1.5$ and Kir2.1 channels to the plasma membrane. Therefore, it seems reasonable to speculate that Kir2.1 mutants that affect trafficking from the endoplasmic reticulum have similar effects. However, while our data uncovers a common

early anterograde trafficking pathway for $Na_V1.5$ and Kir2.1 channels, it is premature to expect that all Kir2.1 trafficking-deficient channels will induce a decrease in I_{Na} density. In this regard, an unexpected finding was that $Na_V1.5^{WT}$ channel failed to rescue mutant Kir2.1$^{\Delta 314–315}$ plasma membrane expression. However, it is possible that for trafficking deficient Kir2.1 mutants with weaker trafficking properties, the presence of $Na_V1.5$ channels might rescue and promote surface expression. It is also possible that trafficking-deficient $Na_V1.5$ mutations affect functional expression of Kir2.1 and other membrane channels. In this regard, it has been shown previously that the α-subunit of I_{Ks} can interact with and modify the localization and current-carrying properties of the α-subunit of I_{Kr}.[64] Clearly additional work is needed to unravel the details of regulation of early trafficking of cardiac ion channels and their incorporation into macromolecular complexes at the cell membrane.

Potential limitations

Our study has potential limitations. First, some experiments were performed in heterologous HEK-293T, COS-7 or CHO cell expression systems, which make interpretation of trafficking studies difficult. However, we validated functional expression results by recording native I_{Na} and I_{K1} as well as AP characteristics in ARVMs and hiPSC-CMs. Second, based on our data we are unable to differentiate whether the observed trafficking disruption in $Na_V1.5$ on Kir2.1$^{\Delta 314–315}$ expression was due to a delay in expression kinetics, or whether all newly synthetized $Na_V1.5$ channels were retained in the Golgi. Third, we cannot rule out that accumulation of trafficking-deficient mutant Kir2.1$^{\Delta 314–315}$ at the Golgi evokes a stress state, and the response to adjust Golgi capacity to myocyte demand might be compromised. Finally, we did not determine whether preferential reduction of $Na_V1.5$ channel was localized to the lateral membrane, T tubules or intercalated discs.

The above limitations notwithstanding, our results provide strong evidence that the $Na_V1.5$-Kir2.1 macromolecular complex preassembles early in its forward trafficking pathway, and that trafficking deficiency and retention of one channel at the Golgi affects trafficking of both channels. Our data also show that $Na_V1.5$ channels may be selected as cargo into Golgi export carriers in a signal dependent manner through an AP1 clathrin adaptor interaction. Altogether, the data provide novel insights into molecular mechanisms underlying arrhythmogenesis in ATS1 patients.

Supplementary Material

Refer to Web version on PubMed Central for supplementary material.

Acknowledgments

We gratefully acknowledge Nulang Wang for technical excellence in isolation and culture of cardiac myocytes. We gratefully acknowledge Yan Chen for technical excellence in the production of the mutant plasmids.

SOURCES OF FUNDING

This work was supported in part by the National Heart, Lung, and Blood Institute (R01 Grant HL122352) and grants from Transatlantic Networks of Excellence Program from the Leducq Foundation, and Fondos FEDER, Madrid, Spain, to J. Jalife. D. Ponce-Balbuena and B. C. Willis were supported by American Heart Association Postdoctoral Fellowships 14POST17820005 and 12POST12030292, respectively. F.J Alvarado was supported by

American Heart Association Predoctoral Fellowship 14PRE19500012 E. Delpón and R. Caballero were funded with Fondos FEDER and Ministerio de Economía y Competividad (SAF2014-58769-P).

Nonstandard Abbreviations and Acronyms

AP	Action potential
AP1	Adaptor protein complex 1
AP2	Adaptor protein complex 2
AP3	Adaptor protein complex 3
AP4	Adaptor protein complex 4
AP5	Adaptor protein complex 5
APD	Action potential duration
ARVM	Adult rat ventricular myocytes
ATS1	Andersen-Tawil Syndrome type 1
CHO	Chine hamster ovary
COS-7	**C**V-1 (simian) in **O**rigin carrying the **S**V40 genetic material
EAD	Early afterdepolarizations
Endo-H	Endoglycosidase-H
ER	Endoplasmic reticulum
FBS	Fetal bovine serum
FRAP	Fluorescence-recovery-after-photobleaching
HEK	Human embryonic kidney
hiPSC-CMs	Human induce pluripotent stem cell derived cardiomyocytes
$\mathbf{I_{K1}}$	Inward rectifier potassium current
$\mathbf{I_{Na}}$	Inward sodium current
$\mathbf{I_{to}}$	Transient outward potassium current
Kir	Inward rectifier potassium channel
MDP	Maximum diastolic potential
$\mathbf{Na_V1.5}$	Voltage-gate sodium channel
PBS	Phosphate buffer saline
PNGase-F	Peptide-*N*-Glycosidase-F

PVCs	Premature ventricular contraction
ROI	Regions of interest
VT	Ventricular tachycardia
WT	Wildtype

References

1. Wang Z, Yue L, White M, Pelletier G, Nattel S. Differential distribution of inward rectifier potassium channel transcripts in human atrium versus ventricle. Circulation. 1998; 98:2422–8. [PubMed: 9832487]
2. Anumonwo JM, Lopatin AN. Cardiac strong inward rectifier potassium channels. Journal of molecular and cellular cardiology. 2010; 48:45–54. [PubMed: 19703462]
3. Nichols CG, Makhina EN, Pearson WL, Sha Q, Lopatin AN. Inward rectification and implications for cardiac excitability. Circulation research. 1996; 78:1–7. [PubMed: 8603491]
4. Vaquero M, Calvo D, Jalife J. Cardiac fibrillation: from ion channels to rotors in the human heart. Heart rhythm: the official journal of the Heart Rhythm Society. 2008; 5:872–9.
5. Cohen AW, Hnasko R, Schubert W, Lisanti MP. Role of caveolae and caveolins in health and disease. Physiological reviews. 2004; 84:1341–79. [PubMed: 15383654]
6. Gaborit N, Le Bouter S, Szuts V, Varro A, Escande D, Nattel S, Demolombe S. Regional and tissue specific transcript signatures of ion channel genes in the non-diseased human heart. The Journal of physiology. 2007; 582:675–93. [PubMed: 17478540]
7. Melnyk P, Zhang L, Shrier A, Nattel S. Differential distribution of Kir2.1 and Kir2.3 subunits in canine atrium and ventricle. American journal of physiology Heart and circulatory physiology. 2002; 283:H1123–33. [PubMed: 12181143]
8. Christe G. Localization of K(+) channels in the tubules of cardiomyocytes as suggested by the parallel decay of membrane capacitance, IK(1) and IK(ATP) during culture and by delayed IK(1) response to barium. Journal of molecular and cellular cardiology. 1999; 31:2207–13. [PubMed: 10640448]
9. Schram G, Pourrier M, Melnyk P, Nattel S. Differential distribution of cardiac ion channel expression as a basis for regional specialization in electrical function. Circulation research. 2002; 90:939–50. [PubMed: 12016259]
10. Farquhar MG, Palade GE. The Golgi apparatus: 100 years of progress and controversy. Trends in cell biology. 1998; 8:2–10. [PubMed: 9695800]
11. Gu F, Crump CM, Thomas G. Trans-Golgi network sorting. Cellular and molecular life sciences: CMLS. 2001; 58:1067–84. [PubMed: 11529500]
12. Ma D, Taneja TK, Hagen BM, Kim BY, Ortega B, Lederer WJ, Welling PA. Golgi export of the Kir2.1 channel is driven by a trafficking signal located within its tertiary structure. Cell. 2011; 145:1102–15. [PubMed: 21703452]
13. Park SY, Guo X. Adaptor protein complexes and intracellular transport. Bioscience reports. 2014:34.
14. Bonifacino JS. Adaptor proteins involved in polarized sorting. The Journal of cell biology. 2014; 204:7–17. [PubMed: 24395635]
15. Paczkowski JE, Richardson BC, Fromme JC. Cargo adaptors: structures illuminate mechanisms regulating vesicle biogenesis. Trends in cell biology. 2015; 25:408–16. [PubMed: 25795254]
16. Catterall WA. Molecular properties of voltage-sensitive sodium channels. Annual review of biochemistry. 1986; 55:953–85.
17. Goldin AL, Barchi RL, Caldwell JH, Hofmann F, Howe JR, Hunter JC, Kallen RG, Mandel G, Meisler MH, Netter YB, Noda M, Tamkun MM, Waxman SG, Wood JN, Catterall WA. Nomenclature of voltage-gated sodium channels. Neuron. 2000; 28:365–8. [PubMed: 11144347]

18. Mercier A, Clement R, Harnois T, Bourmeyster N, Bois P, Chatelier A. Nav1.5 channels can reach the plasma membrane through distinct N-glycosylation states. Biochimica et biophysica acta. 2015; 1850:1215–23. [PubMed: 25721215]
19. Gavillet B, Rougier JS, Domenighetti AA, Behar R, Boixel C, Ruchat P, Lehr HA, Pedrazzini T, Abriel H. Cardiac sodium channel Nav1.5 is regulated by a multiprotein complex composed of syntrophins and dystrophin. Circulation research. 2006; 99:407–14. [PubMed: 16857961]
20. Gillet L, Rougier JS, Shy D, Sonntag S, Mougenot N, Essers M, Shmerling D, Balse E, Hatem SN, Abriel H. Cardiac-specific ablation of synapse-associated protein SAP97 in mice decreases potassium currents but not sodium current. Heart rhythm: the official journal of the Heart Rhythm Society. 2015; 12:181–92.
21. Petitprez S, Zmoos AF, Ogrodnik J, Balse E, Raad N, El-Haou S, Albesa M, Bittihn P, Luther S, Lehnart SE, Hatem SN, Coulombe A, Abriel H. SAP97 and dystrophin macromolecular complexes determine two pools of cardiac sodium channels Nav1.5 in cardiomyocytes. Circulation research. 2011; 108:294–304. [PubMed: 21164104]
22. Milstein ML, Musa H, Balbuena DP, Anumonwo JM, Auerbach DS, Furspan PB, Hou L, Hu B, Schumacher SM, Vaidyanathan R, Martens JR, Jalife J. Dynamic reciprocity of sodium and potassium channel expression in a macromolecular complex controls cardiac excitability and arrhythmia. Proceedings of the National Academy of Sciences of the United States of America. 2012; 109:E2134–43. [PubMed: 22509027]
23. Lowe JS, Palygin O, Bhasin N, Hund TJ, Boyden PA, Shibata E, Anderson ME, Mohler PJ. Voltage-gated Nav channel targeting in the heart requires an ankyrin-G dependent cellular pathway. The Journal of cell biology. 2008; 180:173–86. [PubMed: 18180363]
24. Mohler PJ, Splawski I, Napolitano C, Bottelli G, Sharpe L, Timothy K, Priori SG, Keating MT, Bennett V. A cardiac arrhythmia syndrome caused by loss of ankyrin-B function. Proceedings of the National Academy of Sciences of the United States of America. 2004; 101:9137–42. [PubMed: 15178757]
25. Balijepalli RC, Kamp TJ. Caveolae, ion channels and cardiac arrhythmias. Progress in biophysics and molecular biology. 2008; 98:149–60. [PubMed: 19351512]
26. Matamoros M, Perez-Hernandez M, Guerrero-Serna G, Amoros I, Barana A, Nunez M, Ponce-Balbuena D, Sacristan S, Gomez R, Tamargo J, Caballero R, Jalife J, Delpon E. Nav1.5 N-terminal domain binding to alpha1-syntrophin increases membrane density of human Kir2.1, Kir2.2 and Nav1.5 channels. Cardiovascular research. 2016
27. Utrilla RG, Nieto-Marin P, Alfayate S, Tinaquero D, Matamoros M, Perez-Hernandez M, Sacristan S, Ondo L, de Andres R, Diez-Guerra FJ, Tamargo J, Delpon E, Caballero R. Kir2.1-Nav1.5 Channel Complexes Are Differently Regulated than Kir2.1 and Nav1.5 Channels Alone. Front Physiol. 2017; 8:903. [PubMed: 29184507]
28. Bendahhou S, Donaldson MR, Plaster NM, Tristani-Firouzi M, Fu YH, Ptacek LJ. Defective potassium channel Kir2.1 trafficking underlies Andersen-Tawil syndrome. The Journal of biological chemistry. 2003; 278:51779–85. [PubMed: 14522976]
29. Plaster NM, Tawil R, Tristani-Firouzi M, Canun S, Bendahhou S, Tsunoda A, Donaldson MR, Iannaccone ST, Brunt E, Barohn R, Clark J, Deymeer F, George AL Jr, Fish FA, Hahn A, Nitu A, Ozdemir C, Serdaroglu P, Subramony SH, Wolfe G, Fu YH, Ptacek LJ. Mutations in Kir2.1 cause the developmental and episodic electrical phenotypes of Andersen's syndrome. Cell. 2001; 105:511–9. [PubMed: 11371347]
30. Tristani-Firouzi M, Jensen JL, Donaldson MR, Sansone V, Meola G, Hahn A, Bendahhou S, Kwiecinski H, Fidzianska A, Plaster N, Fu YH, Ptacek LJ, Tawil R. Functional and clinical characterization of KCNJ2 mutations associated with LQT7 (Andersen syndrome). The Journal of clinical investigation. 2002; 110:381–8. [PubMed: 12163457]
31. Donaldson MR, Yoon G, Fu YH, Ptacek LJ. Andersen-Tawil syndrome: a model of clinical variability, pleiotropy, and genetic heterogeneity. Annals of medicine. 2004; 36(Suppl 1):92–7. [PubMed: 15176430]
32. Kaur K, Zarzoso M, Ponce-Balbuena D, Guerrero-Serna G, Hou L, Musa H, Jalife J. TGF-beta1, released by myofibroblasts, differentially regulates transcription and function of sodium and potassium channels in adult rat ventricular myocytes. PloS one. 2013; 8:e55391. [PubMed: 23393573]

33. Stockklausner C, Klocker N. Surface expression of inward rectifier potassium channels is controlled by selective Golgi export. The Journal of biological chemistry. 2003; 278:17000–5. [PubMed: 12609985]
34. Kolb AR, Needham PG, Rothenberg C, Guerriero CJ, Welling PA, Brodsky JL. ESCRT regulates surface expression of the Kir2.1 potassium channel. Molecular biology of the cell. 2014; 25:276–89. [PubMed: 24227888]
35. Kornfeld R, Kornfeld S. Assembly of asparagine-linked oligosaccharides. Annual review of biochemistry. 1985; 54:631–64.
36. Caster AH, Sztul E, Kahn RA. A role for cargo in Arf-dependent adaptor recruitment. The Journal of biological chemistry. 2013; 288:14788–804. [PubMed: 23572528]
37. Eichel CA, Beuriot A, Chevalier MY, Rougier JS, Louault F, Dilanian G, Amour J, Coulombe A, Abriel H, Hatem SN, Balse E. Lateral Membrane-Specific MAGUK CASK Down-Regulates NaV1.5 Channel in Cardiac Myocytes. Circulation research. 2016; 119:544–56. [PubMed: 27364017]
38. Shy D, Gillet L, Ogrodnik J, Albesa M, Verkerk AO, Wolswinkel R, Rougier JS, Barc J, Essers MC, Syam N, Marsman RF, van Mil AM, Rotman S, Redon R, Bezzina CR, Remme CA, Abriel H. PDZ domain-binding motif regulates cardiomyocyte compartment-specific NaV1.5 channel expression and function. Circulation. 2014; 130:147–60. [PubMed: 24895455]
39. Zhou J, Shin HG, Yi J, Shen W, Williams CP, Murray KT. Phosphorylation and putative ER retention signals are required for protein kinase A-mediated potentiation of cardiac sodium current. Circulation research. 2002; 91:540–6. [PubMed: 12242273]
40. Zhou J, Yi J, Hu N, George AL Jr, Murray KT. Activation of protein kinase A modulates trafficking of the human cardiac sodium channel in Xenopus oocytes. Circulation research. 2000; 87:33–8. [PubMed: 10884369]
41. Ma D, Zerangue N, Lin YF, Collins A, Yu M, Jan YN, Jan LY. Role of ER export signals in controlling surface potassium channel numbers. Science. 2001; 291:316–9. [PubMed: 11209084]
42. Stockklausner C, Ludwig J, Ruppersberg JP, Klocker N. A sequence motif responsible for ER export and surface expression of Kir2.0 inward rectifier K(+) channels. FEBS letters. 2001; 493:129–33. [PubMed: 11287009]
43. Zerangue N, Schwappach B, Jan YN, Jan LY. A new ER trafficking signal regulates the subunit stoichiometry of plasma membrane K(ATP) channels. Neuron. 1999; 22:537–48. [PubMed: 10197533]
44. Hofherr A, Fakler B, Klocker N. Selective Golgi export of Kir2.1 controls the stoichiometry of functional Kir2.x channel heteromers. Journal of cell science. 2005; 118:1935–43. [PubMed: 15827083]
45. Herron TJ, Rocha AM, Campbell KF, Ponce-Balbuena D, Willis BC, Guerrero-Serna G, Liu Q, Klos M, Musa H, Zarzoso M, Bizy A, Furness J, Anumonwo J, Mironov S, Jalife J. Extracellular Matrix-Mediated Maturation of Human Pluripotent Stem Cell-Derived Cardiac Monolayer Structure and Electrophysiological Function. Circulation Arrhythmia and electrophysiology. 2016; 9:e003638. [PubMed: 27069088]
46. Zimmer T, Biskup C, Bollensdorff C, Benndorf K. The beta1 subunit but not the beta2 subunit colocalizes with the human heart Na+ channel (hH1) already within the endoplasmic reticulum. The Journal of membrane biology. 2002; 186:13–21. [PubMed: 11891585]
47. Zimmer T, Biskup C, Dugarmaa S, Vogel F, Steinbis M, Bohle T, Wu YS, Dumaine R, Benndorf K. Functional expression of GFP-linked human heart sodium channel (hH1) and subcellular localization of the a subunit in HEK293 cells and dog cardiac myocytes. The Journal of membrane biology. 2002; 186:1–12. [PubMed: 11891584]
48. Yarbrough TL, Lu T, Lee HC, Shibata EF. Localization of cardiac sodium channels in caveolin-rich membrane domains: regulation of sodium current amplitude. Circulation research. 2002; 90:443–9. [PubMed: 11884374]
49. Makara MA, Curran J, Little SC, Musa H, Polina I, Smith SA, Wright PJ, Unudurthi SD, Snyder J, Bennett V, Hund TJ, Mohler PJ. Ankyrin-G coordinates intercalated disc signaling platform to regulate cardiac excitability in vivo. Circulation research. 2014; 115:929–38. [PubMed: 25239140]

50. Bonifacino JS, Traub LM. Signals for sorting of transmembrane proteins to endosomes and lysosomes. Annual review of biochemistry. 2003; 72:395–447.
51. van Bemmelen MX, Rougier JS, Gavillet B, Apotheloz F, Daidie D, Tateyama M, Rivolta I, Thomas MA, Kass RS, Staub O, Abriel H. Cardiac voltage-gated sodium channel Nav1.5 is regulated by Nedd4–2 mediated ubiquitination. Circulation research. 2004; 95:284–91. [PubMed: 15217910]
52. Rougier JS, van Bemmelen MX, Bruce MC, Jespersen T, Gavillet B, Apotheloz F, Cordonier S, Staub O, Rotin D, Abriel H. Molecular determinants of voltage-gated sodium channel regulation by the Nedd4/Nedd4-like proteins. Am J Physiol Cell Physiol. 2005; 288:C692–701. [PubMed: 15548568]
53. Luo L, Ning F, Du Y, Song B, Yang D, Salvage SC, Wang Y, Fraser JA, Zhang S, Ma A, Wang T. Calcium-dependent Nedd4–2 upregulation mediates degradation of the cardiac sodium channel Nav1.5: implications for heart failure. Acta Physiol (Oxf). 2017; 221:44–58. [PubMed: 28296171]
54. Bonifacino JS, Glick BS. The mechanisms of vesicle budding and fusion. Cell. 2004; 116:153–66. [PubMed: 14744428]
55. Boyett MR, Jewell BR. A study of the factors responsible for rate-dependent shortening of the action potential in mammalian ventricular muscle. The Journal of physiology. 1978; 285:359–80. [PubMed: 745095]
56. Boyett MR. An analysis of the effect of the rate of stimulation and adrenaline on the duration of the cardiac action potential. Pflugers Arch. 1978; 377:155–66. [PubMed: 569809]
57. Li GR, Yang B, Feng J, Bosch RF, Carrier M, Nattel S. Transmembrane ICa contributes to rate-dependent changes of action potentials in human ventricular myocytes. Am J Physiol. 1999; 276:H98–H106. [PubMed: 9887022]
58. Lee YS, Hwang M, Song JS, Li C, Joung B, Sobie EA, Pak HN. The Contribution of Ionic Currents to Rate-Dependent Action Potential Duration and Pattern of Reentry in a Mathematical Model of Human Atrial Fibrillation. PloS one. 2016; 11:e0150779. [PubMed: 26964092]
59. Shy D, Gillet L, Abriel H. Cardiac sodium channel NaV1.5 distribution in myocytes via interacting proteins: the multiple pool model. Biochimica et biophysica acta. 2013; 1833:886–94. [PubMed: 23123192]
60. Abriel H. Cardiac sodium channel Na(v)1.5 and interacting proteins: Physiology and pathophysiology. Journal of molecular and cellular cardiology. 2010; 48:2–11. [PubMed: 19744495]
61. Clatot J, Ziyadeh-Isleem A, Maugenre S, Denjoy I, Liu H, Dilanian G, Hatem SN, Deschenes I, Coulombe A, Guicheney P, Neyroud N. Dominant-negative effect of SCN5A N-terminal mutations through the interaction of Na(v)1.5 alpha-subunits. Cardiovascular research. 2012; 96:53–63. [PubMed: 22739120]
62. Noujaim SF, Pandit SV, Berenfeld O, Vikstrom K, Cerrone M, Mironov S, Zugermayr M, Lopatin AN, Jalife J. Up-regulation of the inward rectifier K+ current (I K1) in the mouse heart accelerates and stabilizes rotors. The Journal of physiology. 2007; 578:315–26. [PubMed: 17095564]
63. Donaldson MR, Jensen JL, Tristani-Firouzi M, Tawil R, Bendahhou S, Suarez WA, Cobo AM, Poza JJ, Behr E, Wagstaff J, Szepetowski P, Pereira S, Mozaffar T, Escolar DM, Fu YH, Ptacek LJ. PIP2 binding residues of Kir2.1 are common targets of mutations causing Andersen syndrome. Neurology. 2003; 60:1811–6. [PubMed: 12796536]
64. Ehrlich JR, Pourrier M, Weerapura M, Ethier N, Marmabachi AM, Hebert TE, Nattel S. KvLQT1 modulates the distribution and biophysical properties of HERG. A novel alpha-subunit interaction between delayed rectifier currents. The Journal of biological chemistry. 2004; 279:1233–41. [PubMed: 14585842]

NOVELTY AND SIGNIFICANCE

What Is Known?

- The main cardiac sodium channel ($Na_V1.5$) and the strong inward rectifier potassium channel (Kir2.1) reciprocally modulate their functional expression, an interplay that is crucial to normal cardiac electrical function. By controlling resting membrane potential, IK1 modifies sodium channel availability and therefore cell excitability, APD, and conduction velocity.
- $Na_V1.5$ and Kir2.1 channels physically interact together with multiple other protein partners from early stages of protein trafficking, targeting through membrane anchoring, recycling and degradation.

What New Information Does This Article Contribute?

- A pool of $Na_V1.5$ and Kir2.1 channels preassemble during early forward trafficking and travel together to common membrane microdomains.
- Similar to Kir2.1, some $Na_V1.5$ channels can exit the Golgi apparatus by an adaptor protein complex 1 (AP1)-dependent trafficking process.
- Trafficking deficiency of Kir2.1 channels affects trafficking of both Kir2.1 and $Na_V1.5$ channels complex components, which may have important implications for the mechanisms of arrhythmias in inheritable and possibly other cardiac diseases.

Cardiac $Na_V1.5$ and Kir2.1 function within macromolecular complexes to control cardiac excitability. Cellular processes that regulate trafficking and expression of Kir2.1 and $Na_V1.5$ channels are of interest as potential mediators of proarrhythmic channelopathies and arrhythmogenesis in other cardiac diseases, including heart failure. However, it remains unknown whether Kir2.1 and $Na_V1.5$ pre-assemble or interact during early anterograde trafficking steps of their secretory pathways. Here, we demonstrate that the $Na_V1.5$ and Kir2.1 form a complex that preassembles early in its forward trafficking pathway. Further, we found that $Na_V1.5$ channels may be selected as cargo into Golgi export carriers in a signal dependent manner through an AP1 clathrin adaptor interaction. Moreover, trafficking deficiency and retention of Kir2.1 channel at the Golgi apparatus affects trafficking of $Na_V1.5$ channels. Our data highlight the importance of considering effects of trafficking defective mutations on functional expression of other ion channels or proteins that may be a part of the macromolecular complex within which the proteins interact. Our study offers a novel paradigm regarding the molecular mechanism of arrhythmia susceptibility in monogenic ion channels diseases such as the Andersen Tawil Syndrome and potentially other diseases, including Brugada syndrome.

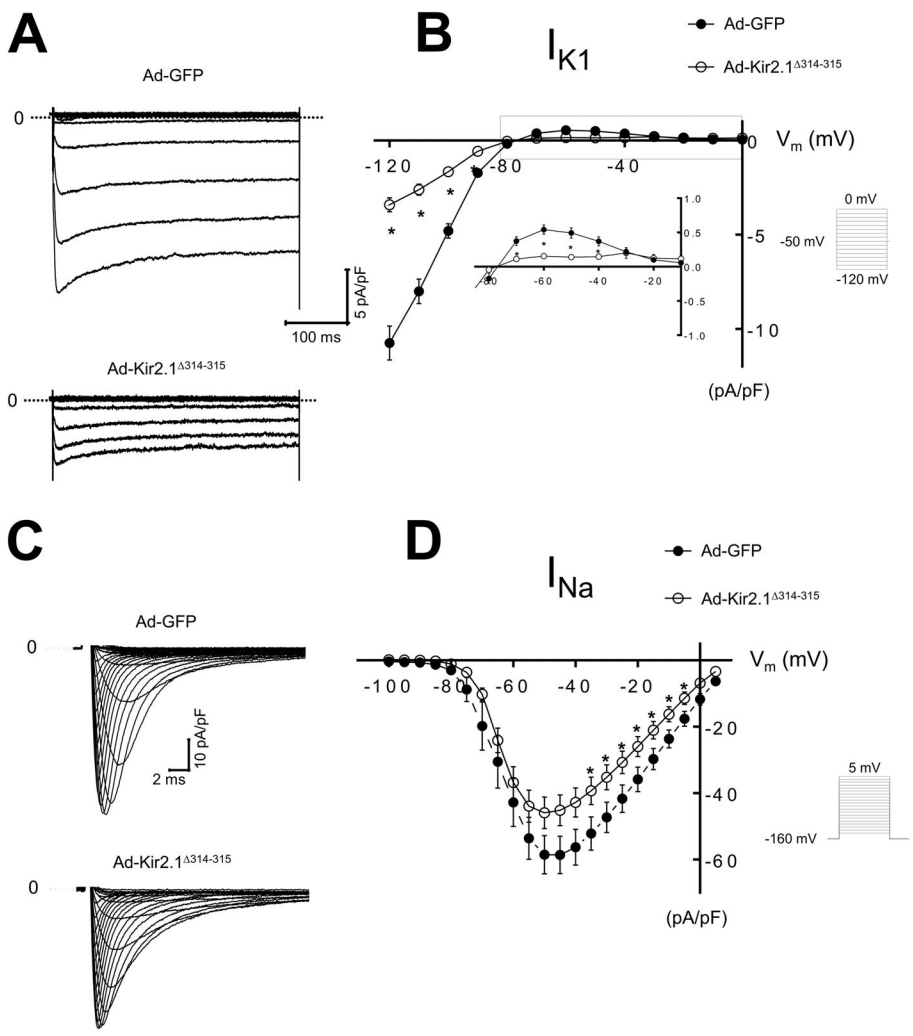

Figure 1. Adenoviral gene overexpression of GFP and Kir2.1$^{\Delta 314–315}$ in ARVMs at 48 h

A. I_{K1} traces from ARVMs infected with Ad-GFP or Ad-Kir2.1$^{\Delta 314–315}$. **B.** I_{K1} I/V relationships for Ad-GFP and Ad-Kir2.1$^{\Delta 314–315}$ (N=4, n=12 and N=6, n=13, respectively). **C.** I_{Na} traces from ARVMs infected with Ad-GFP or Ad-Kir2.1$^{\Delta 314–315}$. **D.** I_{Na}, I/V relationships for Ad- GFP, Ad-Kir2.1$^{\Delta 314–315}$ (N=3, n=12 and N=4, n=10, respectively). *p<0.05, mean±SEM, (t-test). N, number of animals; n, number of cells. Insert describes voltage pulse protocols.

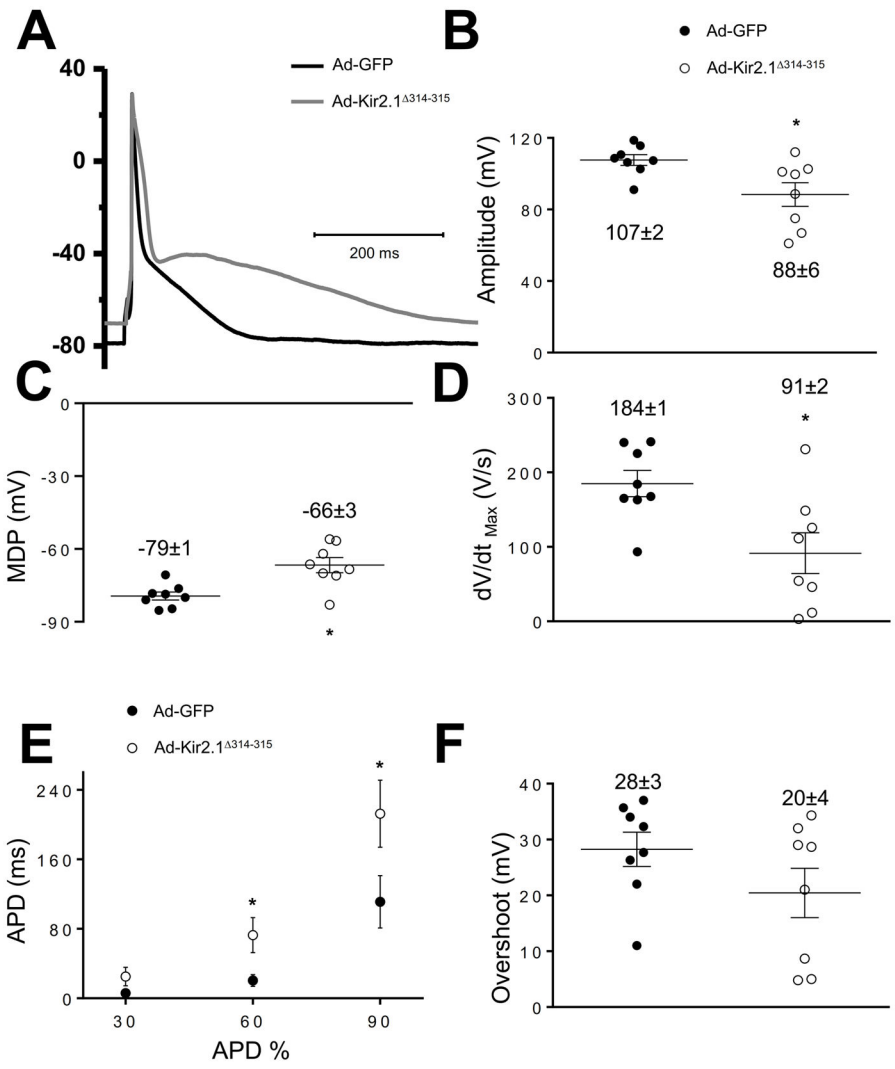

Figure 2. Effect Ad-Kir2.1$^{\Delta 314–315}$ overexpression on action potential characteristics of ARVMs

A. Representative action potential recordings from ARVMs infected with adenoviruses encoding Ad-GFP and Ad-Kir2.1$^{\Delta 314–315}$ at 1 Hz. **B,C,D, E, F** Average amplitude (**B**), maximum diastolic potential (**C**), maximal dV/dt (**D**), action potential duration to 30, 60 and 90% of repolarization (**E**) and overshoot (**F**) (N=3, n=8 and N=3, n=8, respectively, where N is the number of animals and n is the number of cells) *p<0.05, mean±SEM, (t-test).

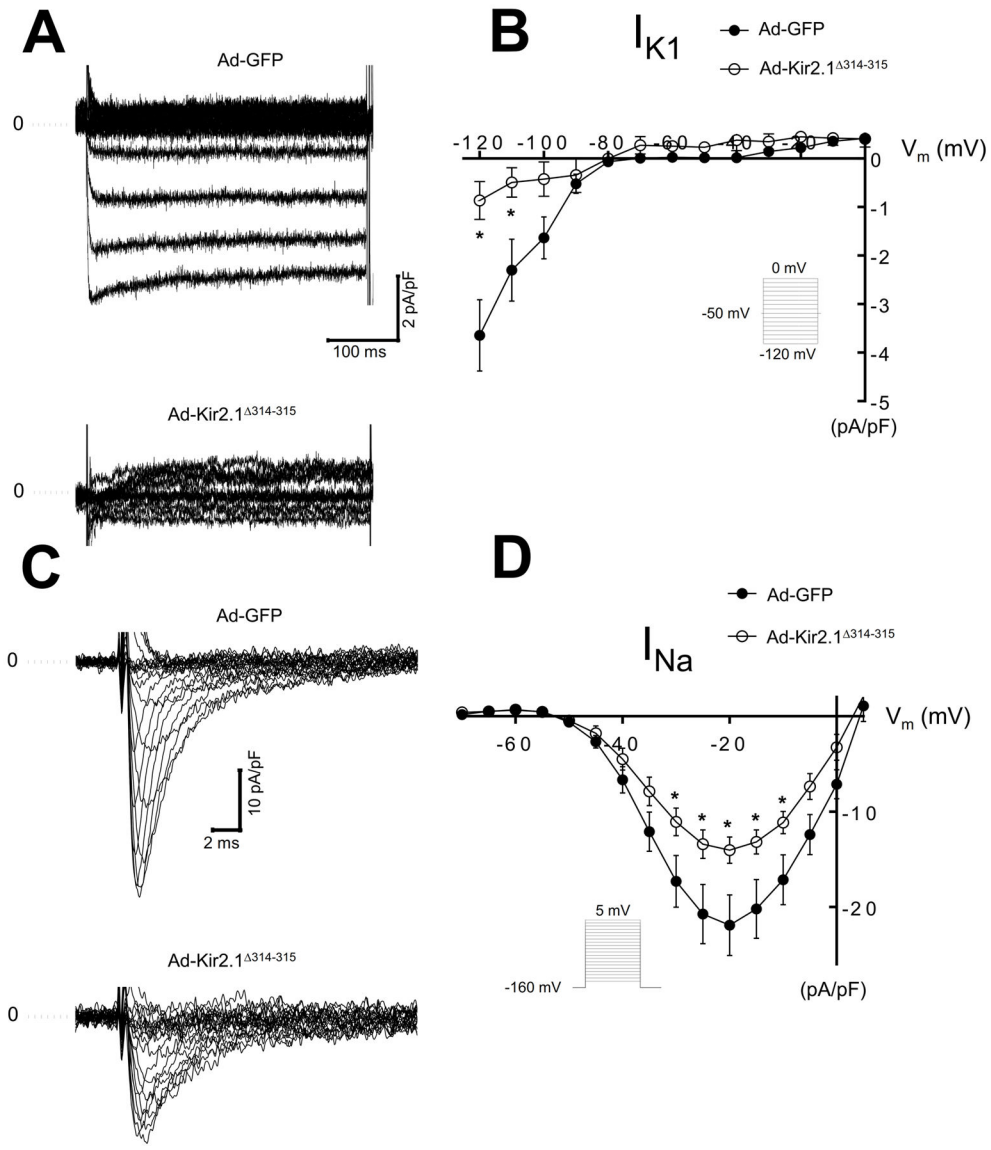

Figure 3. ATS1 mutant Kir2.1$^{\Delta 314–315}$ decreases I_{K1} and I_{Na} density on human induced pluripotent stem cell-derived cardiomyocytes (hiPSC-CMs)

A. I_{K1} traces from hiPSC-CMs infected with Ad-GFP or Ad-Kir2.1$^{\Delta 314–315}$. **B.** Superimposed I_{K1} I/V relationships for Ad-GFP and Ad-Δ314–315 (N=3, n=6 and N=3, n=6, respectively). **C.** I_{Na} traces from hiPSC-CMs infected with Ad-GFP or Ad-Kir2.1$^{\Delta 314–315}$. **D.** I_{Na}, I/V relationships for Ad-GFP, Ad-Kir2.1$^{\Delta 314–315}$ (N=3, n=7 and N=3, n=17, respectively). *p<0.05, mean±SEM, (t-test). N, number of hiPSC-CMs batches infected, n, number of cells. Insert describes voltage pulse protocols.

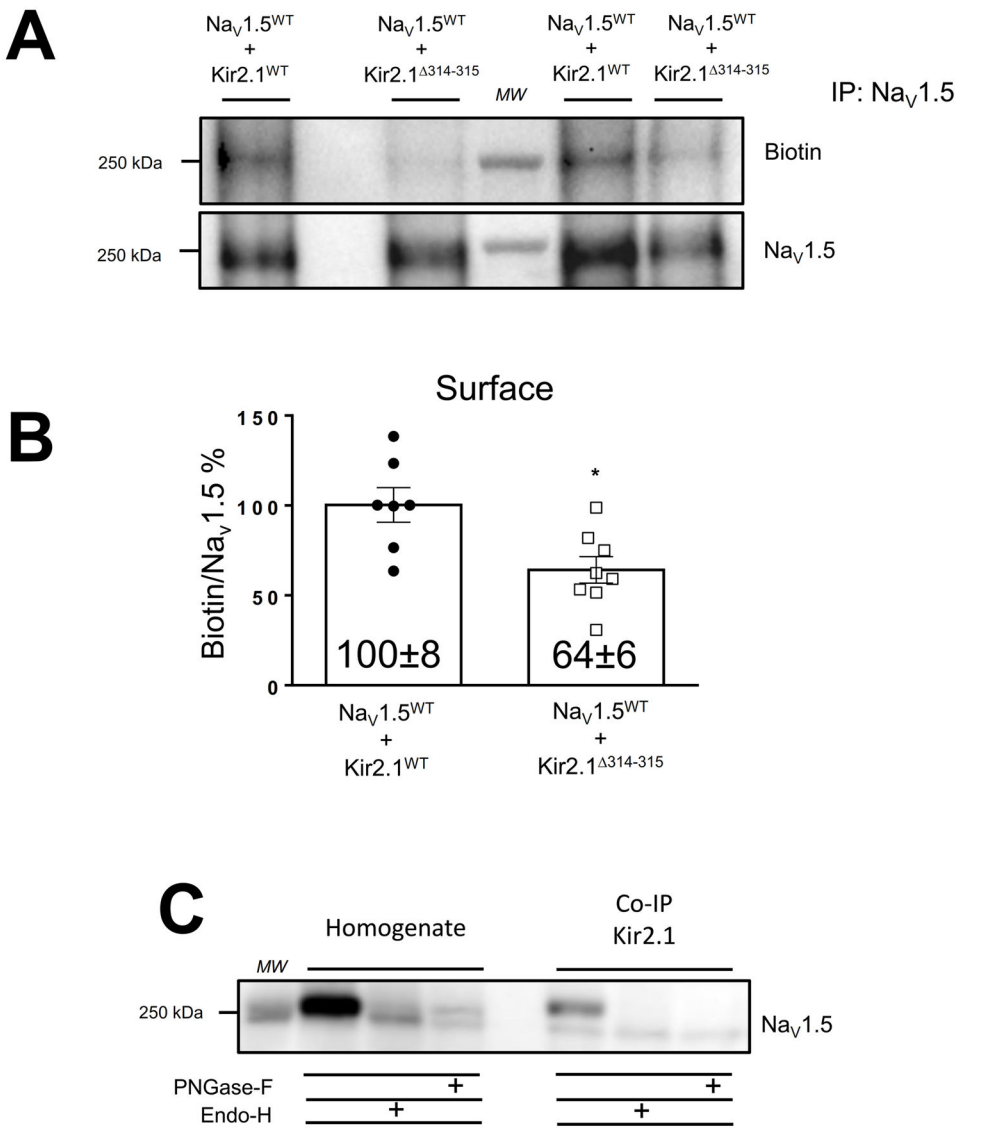

Figure 4. The trafficking deficient mutant $Kir2.1^{\Delta 314–315}$ decreases plasma membrane expression of $Na_V1.5$ channels in HEK-293T cells

A. Representative Western blots of cell surface biotinylation studies. Samples were immunoprecipitated with rabbit anti-$Na_V1.5$ and detected by immunobloting with mouse anti-$Na_V1.5$ and streptavidin HRP conjugated. **B.** Graphic of quantification of $Na_V1.5$ cell surface expression. Cell surface membrane expression of $Na_V1.5$ channels was markedly reduced in the presence of $Kir2.1^{\Delta 314–315}$ compared with $Kir2.1^{WT}$. *p<0.05, mean±SEM, (t-test), ($Na_V1.5^{WT}$+$Kir2.1^{WT}$ (n=7) and $Na_V1.5^{WT}$+$Kir2.1^{\Delta 314–315}$ (n=8), respectively. **C.** Whole-cell inputs of HEK-293T co-transfected 1:1 with $Na_V1.5^{WT}$ and $Kir2.1^{WT}$ incubated in the absence (control samples) or in the presence of endoglycosidase (Endo-H) or peptide *N*-Glycosidase-F (PNGase-F). *Left*, $Na_V1.5^{WT}$ has populations that are Endo-H and PNGase-F sensitive. *Right*, Triton solubilized $Na_V1.5^{WT}$ were first immunoprecipitated with $Kir2.1^{WT}$ and then deglycosylated with Endo-H and PNGase-F. Equal amounts of sample were treated and subjected to 7.5% SDS-PAGE gel electrophoresis. Deglycosylation assay

experiments were performed in five different batches of cells transfected at different days. *MW*, molecular weight.

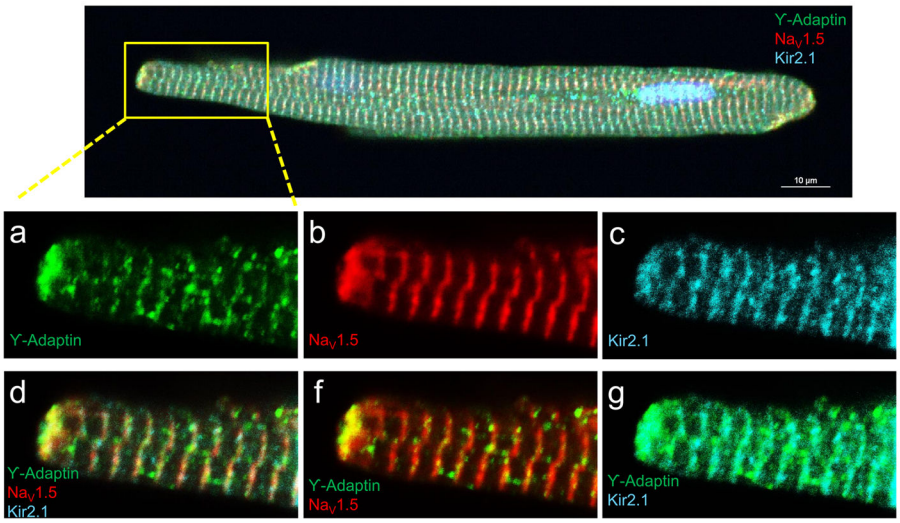

Figure 5. Localization of AP1 ϒ-adaptin, $Na_V1.5$ and Kir2.1 in ARVMs

Top, Overlapping immunostaining for ϒ-adaptin (green), $Na_V1.5$ (red) and Kir2.1 (cyan)**., a,d,** ϒ-adaptin expresses in the t-tubular regions and the intercalated discs. Intense punctate signal densities were also found randomly distributed within the cytoplasm. $Na_V1.5$ and Kir2.1 show similar subcellular distribution at the t-tubules and intercalated discs, **b** and **c,** respectively. ϒ-adaptin, colocalization with $Na_V1.5$ (**f**) and Kir2.1 (**g**)**. d.** Colocalization of the three proteins (Scale bar: 10 μm).

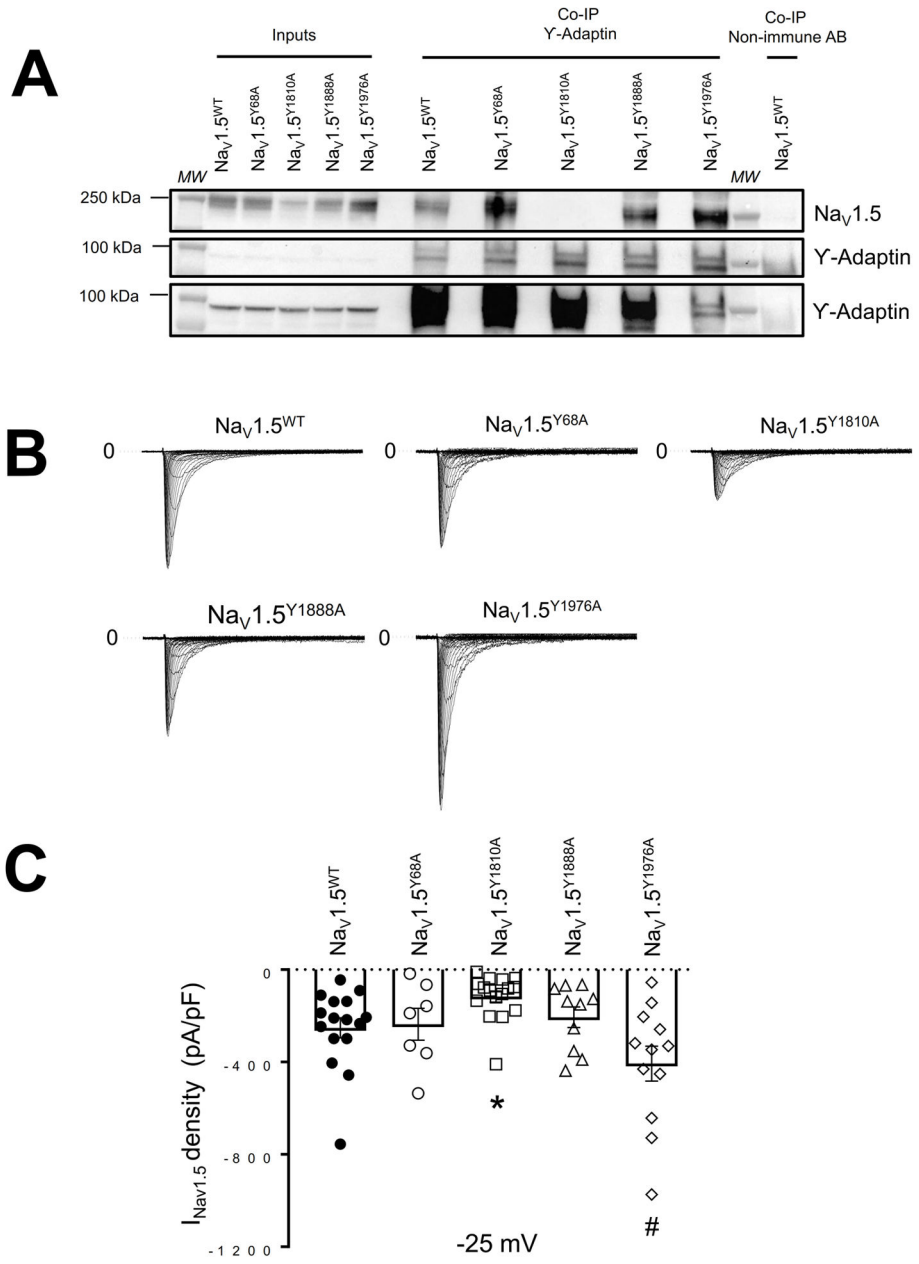

Figure 6. Alanine-scanning mutagenesis of Na$_V$1.5 channels for typical consensus motif to adaptin binding

A. Representative Western blot after immunoprecipitation (IP) with ϒ-adaptin specific antibody. Detected by immunoblot were Na$_V$1.5 and ϒ-adaptin proteins on HEK-293T cells transfected with Na$_V$1.5^{WT}, Nav1.5^{Y68A}, Nav1.5^{Y1810A}, Nav1.5^{Y1888A} and Nav1.5^{Y1976A} (n=3). *Botton* (ϒ-adaptin #) shows a longer exposure of the same immunoblot shown in *Middle*. **B.** Current traces from Na$_V$1.5^{WT}, Nav1.5^{Y68A}, Nav1.5^{Y1810A}, Nav1.5^{Y1888A} and Nav1.5^{Y1976A}. **C**. Peak I$_{Nav1.5}$ density at −25 mV of Na$_V$1.5^{WT}, Nav1.5^{Y68A}, Nav1.5^{Y1810A}, Nav1.5^{Y1888A} and Nav1.5^{Y1976A} (n=16, n=7, n=16, n=10 and n=12, respectively). All constructs/combinations were tested at least in three different batches of

cells transfected in at least three different days. *MW*, molecular weight. *$p<0.05$, $Na_V1.5^{WT}$ *vs* $Na_V1.5^{Y1810A}$, # $p<0.05$, $Na_V1.5^{WT}$ *vs* $Na_V1.5^{Y1976A}$, mean±SEM, Two-way ANOVA.

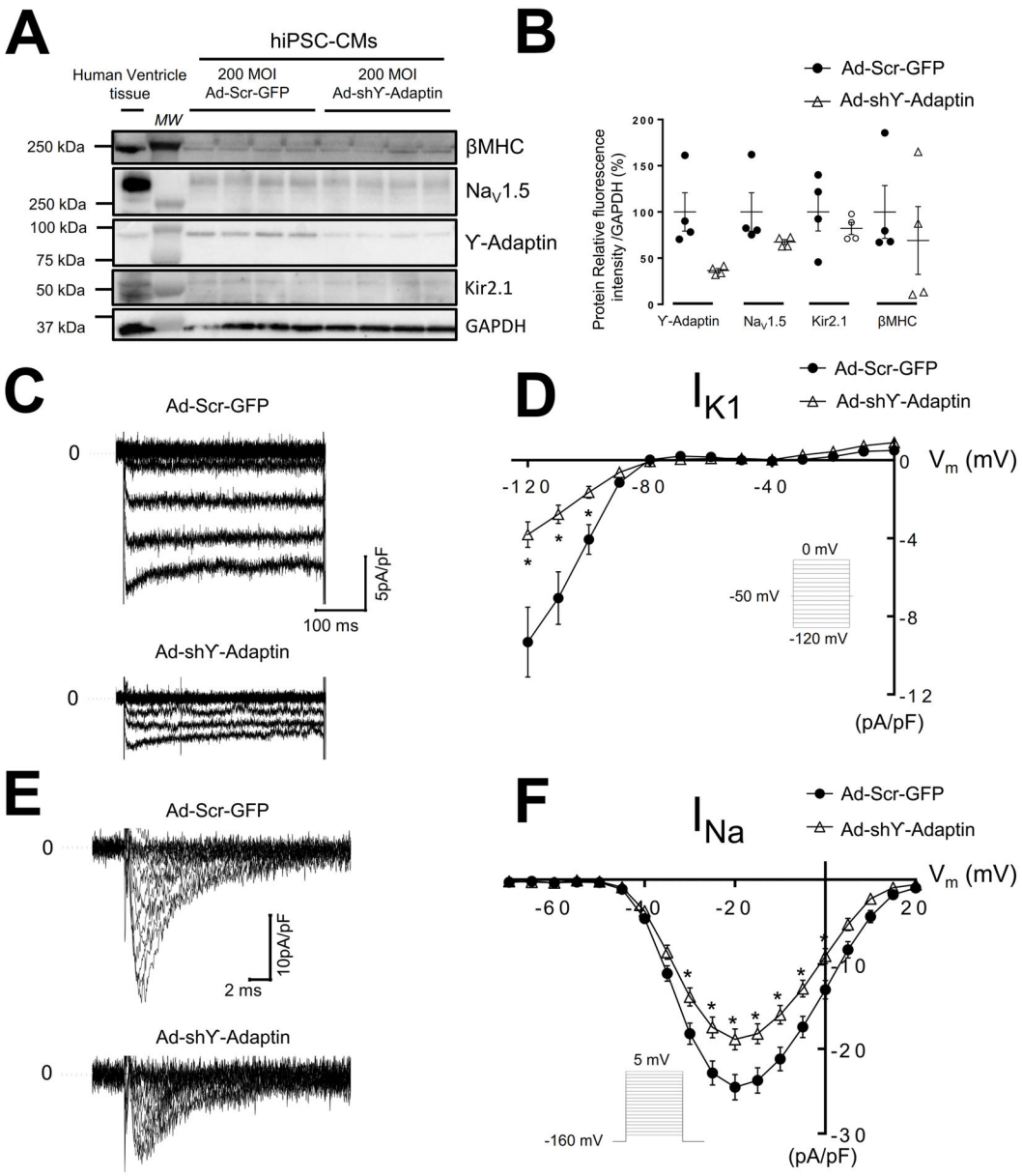

Figure 7. Silence AP1 ϒ-adaptin subunit reduce I_{Na} and I_{K1} on hiPSC-CMs

A, B Ad-shϒ-Adaptin infection silence ϒ-Adaptin subunit on hiPSC-CMs by day 3 in culture monolayers compared with control Ad-Scr-GFP without changing $Na_V1.5^{WT}$, $Kir2.1^{WT}$ and β-cardiac myosin heavy chain (βMHC). **A.** Postinfection Western blot of whole cell preparation of hiPSC-CMs monolayers and human ventricle tissue (100 μg) showing immunodetection of βMHC, $Na_V1.5^{WT}$, ϒ-Adaptin, $Kir2.1^{WT}$ and GAPDH (loading control). **B.** Quantification of ϒ-Adaptin, $Na_V1.5^{WT}$, $Kir2.1^{WT}$ and βMHC, protein expression on whole cell extract from **A. C.** I_{K1} traces from hiPSC-CMs infected with Ad-Scr-GFP or Ad-shϒ-Adaptin, respectively. **D.** Superimposed I_{K1} I/V relationships for Ad-GFP and Ad-shϒ-Adaptin (N =3, n=13 and N=3, n=10, respectively). **E.** I_{Na} traces from hiPSC-CMs infected with Ad-Scr-GFP or Ad-shϒ-Adaptin. **F.** I_{Na}, I/V relationships for Ad-

Scr-GFP, Ad-shϒ-Adaptin (N=3, n=45 and N=3, n=42, respectively). *p<0.05, mean±SEM, (t-test). N, number of hiPSC-CMs batches infected, n, number of cells. Insert describes voltage pulse protocols. *MW*, molecular weight.

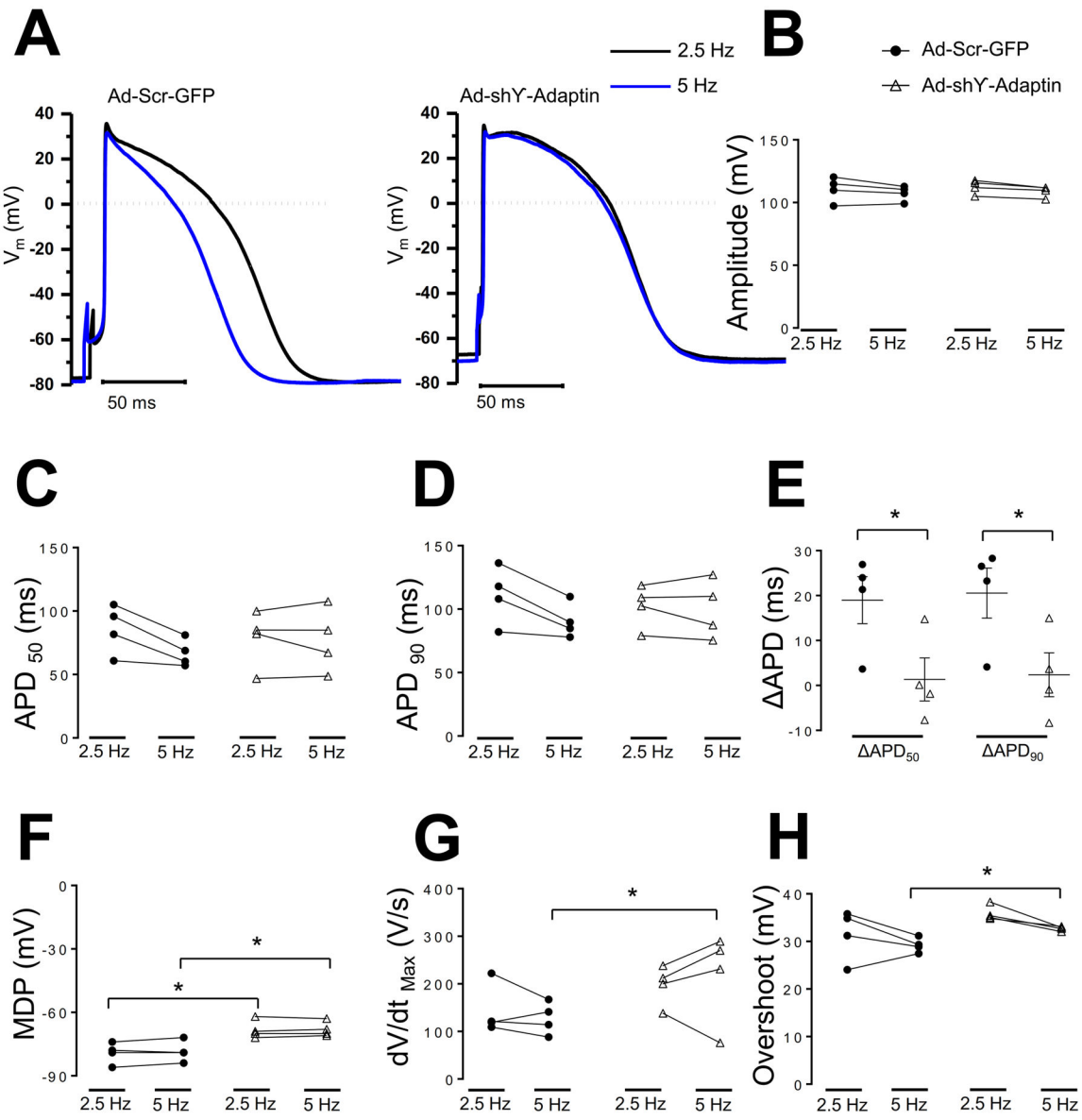

Figure 8. Silence AP1 ϒ-adaptin subunit reduce MDP and impairs rate dependent APD adaptation of hiPSC-CMs

A. Representative action potential recordings from hiPSC-CMs infected with adenoviruses encoding Ad-Scr-GFP and Ad-shϒ-Adaptin at 2.5, 5 Hz (black and blue), respectively. **B,C,D, F, G, H** Plot individual values, amplitude (**B**), action potential duration to 50 and 90% of repolarization (**C**), (**D**), maximum diastolic potential (**F**), maximal dV/dt (**G**), and overshoot (**H**). Delta APD_{50} and APD_{90} repolarization between 2.5 and 5 Hz ($\Delta APD5_{50,\ 90}$) respectively (N=2, n=4 and N=2, n=4, respectively, N, number of hiPSC-CMs batches infected, n, number of cells. *p<0.05, Ad-Scr-GFP *vs* Ad-shϒ-Adaptin mean±SEM, (t-test). Action potential amplitude, overshoot, dV/dt_{max}, APD_{50} and APD_{90} were similar in both hiPSC-CMs groups (112±2, 35±0.6 mV, 229±31 V/s, 78±9 and 81±7 ms in Ad-shϒ-adaptin treated iPSC-CMs *versus* 110±4, 31±2 mV, 142±22 V/s, 85±8 and 88±9 ms in Ad-Scr-GFP treated iPSC-CMs, p>0.05 for Action potential amplitude, overshoot, dV/dt_{max}, APD_{50} and

APD_{90} at 2.5 Hz and (108±1, 32±0.2 mV, 197±18 V/s, 77±1 and 79±9 ms in treated Ad-shϒ-adaptin iPSC-CMs *versus* 107±2, 29±0.6, 127±14 V/s, 66±4 and 72±5 ms, respectively, in Ad-Scr-GFP treated iPSC-CMs, $p>0.05$ for Action potential amplitude, APD_{50} and APD_{90}, $p=0.04$, $p=0.004$ for dV/dt_{max} and overshoot, respectively at 5 Hz.